

UNCLASSIFIED

REPORT

Summary Report No. 1

(Six Month's Summary)

Contracts DA-23-017-AMC-1399(A)

DA-23-017-AMC-1400(A)

29 January 1965

AD 7 9 6 5

PREDICTION OF THE THEORETICAL BEHAVIOR AND ENERGY
TRANSFER WHEN SOLIDS ARE SUBJECTED TO EXPLOSIVE LOADING

COPY	OF	
HARD COPY	\$.	3.00
MICROFICHE	\$.	0.15

231

**UNIVERSITY OF DENVER
DENVER RESEARCH INSTITUTE**

UNCLASSIFIED

DDC
RECEIVED
 APR 13 1965
RECEIVED
 DDC-IRA E

Summary Report No. 1
(Six Month's Summary)

29 January 1965

PREDICTION OF THE THEORETICAL BEHAVIOR AND ENERGY
TRANSFER WHEN SOLIDS ARE SUBJECTED TO EXPLOSIVE LOADING

This Six Month Summary Report, covering the period 29 June 1964 to 29 December, 1964, was prepared under Contract No. DA-28-017-AMC-1399(A), Charge No. 5244-02-802(430) (AED) and Contract No. DA-28-017-AMC-1400(A), Charge No. 5244-02-803(430), AMCMS Code 5545.12.442121

PREPARED FOR:

Commanding Officer
Picatinny Arsenal
Procurement & Production
Directorate, SMUPA-PB
Dover, New Jersey 07801

SUBMITTED BY:

University of Denver
Denver Research Institute
Denver, Colorado 80210

SUBMITTED BY:

Donald C. Tucker
Donald C. Tucker
Project Supervisor
DA-28-017-AMC-1399(A)

PREPARED BY:

Donald C. Tucker
Donald C. Tucker
Research Mathematician

Chester R. Hoggatt
Chester R. Hoggatt
Project Supervisor
DA-28-017-AMC-1400(A)

William R. Orr
William R. Orr
Research Engineer

APPROVED BY:

Rodney F. Recht
Rodney F. Recht
Head, Mechanics Division

Chester R. Hoggatt
Chester R. Hoggatt
Research Metallurgist

FOREWORD

This report was prepared under U. S. Army Contract Numbers DA-28-017-AMC-1399(A) (U) "Investigation of the Transfer of Energy from Explosives to Metal," and DA-28-017-AMC-1400(A) "Prediction of the Theoretical Behavior of Solids Subjected to Explosive Loading," in accordance with Appendix D of the above contracts. The work was under the technical administration of Picatinny Arsenal, Dover, New Jersey, and Contract Administration of St. Louis Procurement District, U. S. Army, St. Louis, Missouri.

Work under sub contract contracts has been running concurrently at Denver Research Institute and many phases of the analyses can be applied to both programs. To eliminate redundancy in the reports and yet to express fully the overall results of both programs, the work has been combined into one report.

This report summarizes the efforts of Denver Research Institute for the first six months of these contracts.

ABSTRACT

A technique to describe the mode of fragmentation and the vector velocity of the fragments from a center initiated cylindrical charge has been proposed in this program. The approach taken permits a determination of these variables from the shape of the case at the instant of breakup. The determination of the shape of the cylinder at various increments of time has been obtained by solving the equations of motion for an explosively loaded cylindrical wall. From the shape of the wall both radial and longitudinal strains can be obtained and a probabilistic method for determining fragment size and number is presented. By considering both the shape and acceleration of the wall at the moment of breakup, a method for obtaining the velocity and direction of the fragments is proposed.

A brief review and discussion of past developments for theoretical and empirical determinations of fragmentation characteristics which include fragment size, number, distribution, and velocity is also presented.

TABLE OF CONTENTS

	<u>Page</u>
FOREWORD	ii
ABSTRACT	iii
TABLE OF CONTENTS	iv
LIST OF FIGURES	v
I. INTRODUCTION AND DISCUSSION OF THE PROBLEM	1
II. LITERATURE SURVEY	3
A. Velocity Determination	3
1. Hydrostatic Models	3
2. Hydrodynamic Models	5
3. Empirical Velocity Measurement and Prediction Techniques	6
B. Fragmentation	7
III. APPROACH TO THE PROBLEM	11
A. Determination of Velocity	12
B. Determination of the Shape of Casing During Expansion	24
C. Determination of Fragment Distribution and Size	29
1. Determination of Strain	29
2. Application of Statistics to the Method of Breakup	31
3. Method of Breakup	36
APPENDIX A - THE GURNEY EQUATION	41
TAYLOR'S THEORY FOR END INITIATED CYLINDERS	50
CYCLONE PROGRAM	51
APPENDIX B - FLAT PLATE ANALYSIS	55
BIBLIOGRAPHY	65

LIST OF FIGURES

<u>Figure No.</u>		<u>Page</u>
1.	Diagram for the Determination of the Radial Motion Equation	13
2.	Velocity Versus Radius of the Cylinder In Terms of Dimensionless Variables	17
3.	Radius of the Cylinder Versus Time in Terms of Dimensionless Variables	18
4.	Velocity of the Cylinder Wall Versus Time in Terms of Dimensionless Variables	19
5.	Velocity of the Cylinder Wall at Various Positions Along the Cylinder for Four Different Time Increments	20
6.	Variation of the \sqrt{F} (Proportional to Velocity) Versus Radius of Cylinder for Various Values of the Specific Heat Ratio (γ)	22
7.	Variation of Velocity Versus Radius of the Cylinder as a Function of the Initial Pressure	23
8.	Determination of Cylinder Shape as a Function of Time	25
9.	Schematic for Determination of the Time of Arrival of the Detonation Front at the Cylinder Wall	27
10.	Radius of the Cylinder at Various Positions Along the Cylinder Wall for Four Different Time Intervals	28
11.	Path of Particles Within the Casing Wall as a Function of Time	30
12.	Probability of Fracture as a Function of Strain	33
13.	Schematic of Fragmentation Process for a Uniformly Stressed Section	38
A-1	Schematic Representation for One Dimensional Expansion Process	42
A-2	Schematic Representation for Two Dimensional or Cylindrical Expansion Process	44

LIST OF FIGURES (Cont.)

<u>Figure No.</u>		<u>Page</u>
A-3	Schematic Representation for Three Dimensional or Spherical Expansion Process	48
B-1	Flat Plate Schematic	56
B-2	Velocity of an Explosively Accelerated Flat Plate Versus Distance of Travel	59
B-3	Distance of Travel Versus Time for an Explosively Accelerated Flat Plate	60
B-4	Velocity of an Explosively Accelerated Flat Plate Versus Time	61
B-5	Schematic of the Shape of a Flat Plate Due to Center Point Initiation of the Explosive	63
B-6	Variation of the $\sqrt{F^t}$ (Proportional to Velocity) Versus Distance of Travel of Flat Plate for Various Values of Specific Heat Ratio (γ)	64

I. INTRODUCTION AND DISCUSSION OF THE PROBLEM

A detailed description of the method of breakup and the characteristics of fragmenting shell and/or bomb casings has been found to be quite difficult to express analytically. The problem has been studied by numerous investigators, but an exact theoretical analysis is quite difficult due to the large number of parameters and variables involved. For this reason, the existing equations which are normally used to describe fragmentation and velocity characteristics are of the empirical or semi-theoretical type, and predict results only for the specific type shell used in obtaining the correlation data.

At the present time the selection of materials or configurations for warhead design are based upon engineering estimates of this type followed by a large amount of testing. The ability to theoretically predict the behavior of various solid media or combinations thereof, under the influence of explosive loading would reduce the amount of fabrication and testing that is presently necessary in the design of any warhead.

The basic purpose of these two programs is to conduct fundamental studies on the behavior of solids subjected to explosive-induced shocks, where the solids are adjacent to the explosive charge. The objective of the overall study is the formulation of a technique which would allow (1) calculation of pressures and lengths of shock waves transmitted into and within solids, (2) prediction of the type and magnitude of deformation and fracture of solids and, (3) calculation of the vector velocity of the explosively accelerated solid fragments.

In the present study the explosive-solid interaction has been separated into three general areas to describe the motion of a solid wall as it is accelerated by the explosive impulse. The first area involves the shock wave interactions due to the initial detonation shock front produced in the solid wall. The second area involves the expansion of the explosive products and the casing wall out to the point of fracture. The third area takes into account the contributions to the fragment velocity due to the gaseous explosion products escaping past the fragments after breakup of the casing. Since preliminary considerations have shown the effects due to the initial interaction to be secondary (in comparison to those occurring in the second area), this area has been given only limited attention in the initial calculations. Contributions related to the third area mentioned above have been considered negligible

up to this time, since it is believed that the escaping gas will probably have no other effect than to maintain the initial velocity attained by the fragments upon breakup until it is sufficiently dissipated to allow air drag to begin the slowing down process. The second area mentioned has therefore received the majority of attention in the study up to this time. It has been expanded to include the actual method of breakup as well as the expansion characteristics of the explosive and the casing. It is felt that if an accurate description of the shape of the casing as a function of time can be determined, then a statistical method somewhat similar to that proposed by N. F. Mott¹ can be used to predict the number and size of fragments for various geometries. The velocity and direction can also be determined from the acceleration and shape of the casing at the moment of breakup, by a method similar to that described by G. I. Taylor.²

While considerations to date have involved only well defined symmetrical cases with centerpoint initiation, future considerations will involve such factors as geometry of the case, material properties, explosive characteristics, buffers, cavities in the explosive charge, wave shape, line and surface initiation, non-steady state detonation rates, and various solid materials including metals, plastics, porous media, and powder aggregates. A detailed investigation of the effects caused by all of the before mentioned items will be some time in coming, but through continued studies such as the ones reported on here much insight on the problems which exist can be realized.

The final outcome of the current contracts will hopefully result in a handbook type report which could be used by a design engineer to make predictions in various practical ordnance applications. However, if the complexity of the program grows to such an extent that this is not possible, the results will be presented in a form suitable for solution on a high speed computer.

II. LITERATURE SURVEY

Perhaps the most complete compendium and bibliography on explosives is in the collection of papers used for the graduate study program at Stevens Institute of Technology. Picatinny Arsenal. on "Detonation Phenomena", 1957-1958. All phases of the phenomena are examined in some detail.

Other important publications related to detonation theory include:

- 1) A paper on "The Stability of Detonation" by Henry Eyring, R. E. Powell, G. H. Duffy and R. B. Parlin. Chemical Reviews, 1949.
- 2) "Behavior of Metals under Impulsive Loads," J. S. Rinehart and J. Pearson, 1954.
- 3) "Stress Waves in Solids," H. Kolsky, 1953.
- 4) "The Science of High Explosives," M. A. Cook, 1958.

The remainder of the literature which was surveyed has been broken down into specific topics of interest. i. e. , velocity and fragmentation and are listed in a bibliography at the end of the report.

A. Velocity Determination

Several proposed theoretical methods and empirical formulas have been developed to determine fragment velocities from explosively loaded systems. Two distinct theoretical models are generally proposed, with the assumptions that the process is either hydrostatic or hydrodynamic in nature. Empirical formulas usually make use of and extend the theoretical models for particular bomb or shell configurations.

1. Hydrostatic Models

Perhaps the most notable contribution to date for the prediction of initial fragment velocity has been by Ronald W. Gurney,³ using a hydrostatic model for spherical and cylindrical configurations. See Appendix A. Theodore E. Sterne⁴, L. H. Thomas⁵, G. W. Atkinson⁶, and E. E. Jones⁷, have extended the hydrostatic models to other configurations. Only three variables are necessary to describe the mean initial velocity

of the fragments in these models, i. e. , mass of charge, mass of case, and a term which represents the explosive $\sqrt{2E}$, where E is defined as the effective energy per unit mass of charge. The constants in the resultant equations are determined by the geometrical configuration and, therefore, geometrical parameters are implicit in the form of the equations.

For example, the equations used to determine the velocity of fragments for the following configurations take the form shown:

- a. A Sphere with uniform casing

$$V_0 = \sqrt{2E} \sqrt{\frac{C/M}{0.6 (C/M) + 1}}$$

- b. An infinite cylinder with uniform casing

$$V_0 = \sqrt{2E} \sqrt{\frac{C/M}{0.5 (C/M) + 1}}$$

- c. A uniform cylinder with identical end plates

$$V_{\text{end plates}} = \sqrt{2E} \sqrt{\frac{6C}{C(2+3K^2)+6K^2M_s+12M_e}}$$

$$V_{\text{cyl}} = KV_{\text{end plates}}$$

$$K = \frac{\rho_e t_e}{\rho_s t_s} \quad \rho_e, \rho_s = \text{density of end plate and cylinder respectively.}$$

$t_e, t_s =$ thickness of end plates and cylinder respectively.

$M_e, M_s =$ Mass of end plates and cylinder respectively.

The size, number and direction of movement of the fragments can not be obtained from the above models. The velocity is assumed to be normal to the defined surfaces and therefore cannot take into account the effects of position of initiation, end and corner effects, bursting strength of the casing, etc.

The usual method used to analyze asymmetric charges, using Gurney type equations, is to divide the case into uniform sections and ascribe to each section that portion of the explosive charge which is in

direct contact with it. These data are then inserted into the appropriate formula (cylinder, sphere, etc.) to determine the fragment velocity corresponding to the given section.

In the paper by E. E. Jones⁷, a method is presented for adjusting the fragment velocity when voids, space for fuzes and other compressible foreign bodies are included in the charges. This involves calculating a correction factor which is multiplied by the uniform case velocity to give a corrected velocity value. The correction factor is found by,

$$F = \sqrt{\frac{(\gamma - 2) + \left(\frac{v_c}{v_c + v_d}\right)^{\gamma - 1}}{\gamma - 1}}$$

where v_c is volume of the charge, v_d is volume of void and γ is the ratio of the specific heat at constant pressure to that at constant volume. Normally a value of $\gamma = 2.75$ to 3.0 is used for explosive gases.

2. Hydrodynamic Models

G. I. Taylor² developed a theoretical hydrodynamic model to represent the expansion of an incompressible cylinder where the detonation products behave as an adiabatically expanding polytropic gas. If the explosive is placed in a long heavy cylindrical casing and initiated at one end, a model is formed wherein the expansion of the gases occurs without the formation of shock waves other than the detonation wave itself. For these conditions the magnitude and direction of the fragments can be found using Taylor's Model. Experiments by Singh⁸, Allison, et al.,⁹ H. Jones¹⁰, have shown that Taylor's relation holds relatively well for several end initiated configurations.

J. Von Neumann and R. D. Richtmyer¹¹ modified the hydrodynamic equations to include additional terms which simplified the numerical solution of the equations for problems involving shocks. Kolsky, Evans, Harlow, (see reference 12), Gleyzal, Solem, Sternberg¹², and Orlow, Piacesi, Sternberg¹³, extended the work of Von Neumann & Richtmyer to two-dimensional or cylindrical-shaped cased-charges. A computer program was developed which aided in the numerical solution of the problem and provided results which compared favorably with experimental data. Dr. Collins of Picatinny Arsenal is presently working on improvements of the above models. The disadvantages of these latter models are their complexity, high cost to run a single analysis.

and the limiting number of data points they can handle before flooding the computer. Storage capacity would be particularly important if inert materials (buffers, wave shapers, etc.) were included in the matrix.

3. Empirical Velocity Measurement and Prediction Techniques

Techniques which are employed for the determination of velocities of fragments from specific shell or bomb configurations include: photographic (also radiographic), electronic, mechanical (penetration capability), modifications of theoretical equations (such as Gurney's equations), etc.

In order to exclude the inaccuracies associated with measurement of small movements, many of the resultant velocities obtained are averages over relatively large distances (one to over a hundred feet). In these instances air drag correction factors must be applied to obtain initial fragment velocities.

Radiographic and photographic coverage has been obtained for a great number of explosive configurations from initiation and for several microseconds thereafter. In order to obtain a time sequence of events, several identical shots must normally be run with appropriate timing. An added problem associated with photographic techniques per se, is that the high intensity light given off by the explosive gases when the case breaks soon obscures the fragment movement. Even with radiographic procedures, the path of a particular fragment cannot be followed; however, the general direction of fragments from a given area of the casing can be obtained. Personnel from Ballistics Research Laboratory, as well as others have been and are presently performing studies of this type.^{14, 15, 16, 17} Personnel from Naval Ordnance Laboratory and Denver Research Institute have recently developed procedures for obtaining sequence pictures of detonating explosives using high-speed framing camera techniques.

A convenient velocity measuring technique utilizes impact and penetration data.^{18, 19} Fragment sizes and distribution data are also readily obtained in such tests with the added feature that the test need not necessarily be static.^{20, 21}

B. Fragmentation

The following survey of literature discusses some of the more generally accepted equations, of both the empirical and semi-theoretical type, which are generally used to define the fragmentation characteristics from shell or bomb cases. The discussion also includes the basic analyses of several authors whose work is applicable to the approach taken in this contract.

Equations adopted by most workers for calculating fragment mass distributions over varying ranges of mass, consist of one of the following forms of the Mott type equations.

$$A) \quad N_m = N e^{-m/\mu}$$

$$\text{giving } M_m = N(m + \mu) e^{-m/\mu}$$

$$B) \quad N_m = N e^{-(m/\mu)^{\frac{1}{2}}}$$

$$\text{giving } M_m = N \left[m + 2 \left(\frac{m}{\mu} \right)^{\frac{1}{2}} + 2\mu \right] e^{-(m/\mu)^{\frac{1}{2}}}$$

$$C) \quad N_m = N e^{-(m/\mu)^{\frac{1}{3}}}$$

$$\text{giving } M_m = N \left(m + 3m^{\frac{2}{3}} \mu^{\frac{1}{3}} + 6m^{\frac{1}{3}} \mu^{\frac{2}{3}} + 6\mu \right) e^{-(m/\mu)^{\frac{1}{3}}}$$

Where N_m and M_m are the number and mass of fragments having a mass greater than m , N and M are the total number and total mass of the fragments, e is the numerical value of the base of Napierian logarithms, m is the individual fragment weight, and μ is a constant.

Formula A, applies for random or semi-random breakup of a bar and is observed to hold well for the larger fragments of fragmentation bombs. Formula B applies for breakup of a thin metal shell and is observed to hold for two-dimensional breakup. Since nearly all service projectiles have wall thicknesses less than 0.6 inches, this equation expresses the fragment distribution obtained from most bombs and artillery shell. Formula C applies for a very thick metal shell and is observed to hold for three-dimensional breakup. This equation may be expected to hold for the smallest fragments of any shell or bomb, since a large number of fragments will be present whose size is not influenced

by the thickness of the casing. When this occurs the mechanism of fragmentation may be more nearly the result of a three-dimensional effect.^{22, 23}

Another equation used for calculating fragment mass distributions is the one developed by Payman and stated as follows:

$$M_m = M e^{-m/\mu}$$

where M_m is the mass of fragments having a mass greater than m . M is the total mass of the fragments,

$$\text{giving } N_m = \frac{M}{\mu} \left[-\text{Ei} \left(-\frac{m}{\mu} \right) \right]$$

$$\text{where } -\text{Ei}(-X) = \int_x^{\infty} \frac{e^{-x}}{x} dx$$

This formula appears to hold for a wider range of cases than Formula B, but provides less accurate results in cases where Formula B is best adapted.

A method which takes into account statistical fluctuations in the data and provides a technique for fitting one of the above semi-theoretical mass distribution formulas to a collection of fragments has been developed by Thomas.^{5, 20, 22} Theoretical reasons are given for a Poisson type fluctuation, and various methods of fitting the equation were examined with this in mind. It was concluded, in the referenced report, that if the masses of all the fragments were measured, the formulas could be fitted by the method of maximum likelihood. If, however, the fragments were divided into large weight groups, parameters of the most suitable form could be chosen to fit the total number and total mass of fragments heavier than the least mass above which all fragments were collected.

A difficulty in analyzing fragmentation data is the non-uniform behavior of the projectiles. There is usually a considerable variation in the number of fragments produced by various shell from the same lot number. A table contained within a report by Gurney²³ lists the average number of fragments of mass greater than m for various type shell and the standard deviation obtained through repeated firings. The deviations reported were considerable (on the order of ± 9 to ± 50 percent). It was

also pointed out that tests conducted at different times between two different explosives in similar metal casings do not yield anything near a constant ratio corresponding to the relative efficiencies of the two explosives; in one test similarity of performance may be present, while in another test a wide difference in fragmentation efficiency exists. With findings of this nature, Gurney, concluded that no more than a rough agreement could be made between experimental fragmentation data and the semi-theoretical formulas.

The equation of form $N_m = N_t e^{-(m/\mu)^{\frac{1}{2}}}$ was further investigated by Tomlinson²⁴ following a time period which witnessed the accumulation of a large amount of accurate data on the fragmenting power of castable high explosives. The investigation revealed that the total number of fragments calculated, according to the equation, and the total number of fragments observed agreed within limits having the same order as the spread of the data within itself.

Using the hydrodynamic theory of detonation, a straight line relation was derived between N_t and $\rho^{\frac{1}{2}} D$, as well as m_a and $\rho^{\frac{1}{2}} D$. Where ρ is the density and D the rate of detonation of the explosive, and m_a the average fragment weight. Both of these relations cannot be straight line expressions, due to the fact that $N_t m_a$ is the shell weight, and the equation $N_t m_a = \text{constant}$ is of hyperbolic form. The straight line relation to $\rho^{\frac{1}{2}} D$ appears to be obeyed better by m_a than N_t . However, the error caused by assuming the hyperbolic relation to be that of a straight line is of the same order as the accuracy of the data involved. By plotting the experimental fragmentation data for specific shell configurations against $\rho^{\frac{1}{2}} D$ values for various explosives, a least squares curve may be obtained which provides a way of comparing the fragmentation efficiency for various explosives.

Since the development of Equation B a completely empirical relation between fragment weights and numbers was published by the Safety in Mines Research Station in Buxton, England²⁴. The relation may be stated as

$$m = \frac{2-p}{C}, \text{ or}$$

$$W_m = W_0 e^{-Cm \ln 10}$$

Where W_0 is the shell weight, W_m the total weight of fragments of individual weight greater than m , $p = \log \frac{100W_m}{W_0}$, and C a constant. This

relation permits a simple analysis of fragmentation data in a much shorter time than was before possible. The equation has been checked against numerous known distributions, but its use for a series of different explosives has not been investigated. The value of this relation lies in the saving of time made possible in the data analysis and the small improvement in fit as compared to Equation B.

A theoretical basis for the prediction of the mass distribution of fragments from shell or bomb cases has been proposed by Mott¹. The theory pertains to the breakup of a cylindrical ring-bomb, where the wall of the shell consists of a number of coaxial circular rings, all with the same inner and outer radii, stacked one above the other around a thin steel inner lining. Each ring breaks into a number of pieces with the planes of fracture parallel to the axis of the cylinder.

The analysis concentrates on only radial fractures and does not attempt to define a complete theory of fragmentation for solid cylinders. The statistics for defining the average size of the fragments from a shell case of a ductile metal depends upon a property of the metal which is not usually measured, namely, the scatter in the values of the strain at which fracture occurs in a tensile test. There is in any length of the circumference of the ring a finite probability of fracture which increases rapidly as the strain approaches some critical value. As soon as fracture occurs at one point, stress is relieved in both directions away from the break and the unstressed regions spread with a velocity which can be calculated. Fracture can no longer take place in the unstressed regions, but within the stressed regions plastic flow is still continuing so the strain is increasing within these regions and fracture becomes more and more likely. The average size of fragment is determined by the rate at which the stress relief waves spread to prevent further fractures. Famiglietti²⁵ has studied ring type bombs made with various metals having widely different physical properties. A more complete discussion of this analysis is contained in Section III of this report.

III. APPROACH TO THE PROBLEM

In order to predict the dynamic behavior of an explosive-solid interaction, it is first necessary to describe the manner in which the solid materials are loaded by the explosive shock wave and the subsequent detonation pressure. Following this it is just as important to know how the solid materials will respond to the loading conditions imposed. Consequently, a designer who wishes to control the dynamic characteristics of a warhead must utilize techniques which have been formulated from solid state wave mechanics and the dynamic behavior of materials.

As previously mentioned, this study has considered the explosive-solid interaction as being composed of three general areas which describe the motion of a solid wall as it is accelerated by an explosive impulse. Two of these areas have been considered secondary up to this time and the primary effort has been concentrated on the expansion of the explosive products and the casing wall out to the point of fracture.

Prior to considering in detail, the mechanisms by which acceleration may occur and the variables and parameters which will be involved, consider the basic laws which govern the motion of any body. An elemental portion of a wall having mass, dm , will be acted upon by external forces which when summed will produce the resultant vector, dF . These forces may act to deform the materials both elastically and plastically. The work accomplished on the body by these forces may cause changes in kinetic energy and/or changes in internal energy; in addition, heat will be produced during irreversible deformation processes when they occur. Irregardless of the energy processes involved, the following relation will always describe the change in momentum experienced by the elemental mass.

$$dVdm = dFdt \quad (1)$$

Consequently, whether the body is rigid or not, the change in velocity of its center of mass will be related directly to the impulse $dFdt$. Dividing both sides of the equation by the constant, dm , and integrating between limits of V_0 and V_1 and t_0 and t_1 gives the total change in velocity during the indicated time period.

$$V_1 - V_0 = \int_{t_0}^{t_1} \frac{dF}{dm} dt \quad (2)$$

The value of the total impulse represented by the right side of the equation determines the magnitude of the velocity change.

If the differential force, dF , acting on the wall element, dm , could be defined in terms of dynamic, geometrical and material parameters with respect to time, Equation (2) would represent the complete solution to the problem. This integral could then be solved and the velocity vector obtained. Replacing dF by the indicated functions of the related parameters would appear to represent quite a chore. Certainly, a completely general solution would be almost out of the question. However, specific types of the general problem will yield more readily to closed solutions.

The initial problem considered in this program is the symmetrical explosive expansion of a ring segment of a thin cylindrical wall, shown in Figure 1. Shock waves introduced in the wall by the variable internal pressure, p , will move back and forth through the wall; however, as noted above the average radial velocity of the wall will be a function only of the impulse $\int p dA dt$.

Since the expansion is symmetrical, all elements, dm , will be accelerated in the same manner. The free-body diagram in Figure 1 illustrates the external forces acting on a wall element. The elemental force, $P r d\theta$, due to the explosive is opposed by the body force $\ddot{r} dm$ (where \ddot{r} is radial acceleration) and the components of the hoop forces, $\sigma (R-r)$, which act in the radial direction. Writing the force balance, and observing that in the limit, $\sin \frac{d\theta}{2} = \frac{d\theta}{2}$, results in the following equation of motion,

$$\ddot{r} = \frac{2 P r - 2 \sigma (R - r)}{\rho (R_0^2 - r_0^2)} \quad (3)$$

This equation will serve as the basis for the following analysis of explosively loaded uniform cylinders.

A. Determination of Velocity

Using the equation of motion for a cylindrical ring (3), equations have been developed for determining the velocity and change in radius of the ring as a function of time.

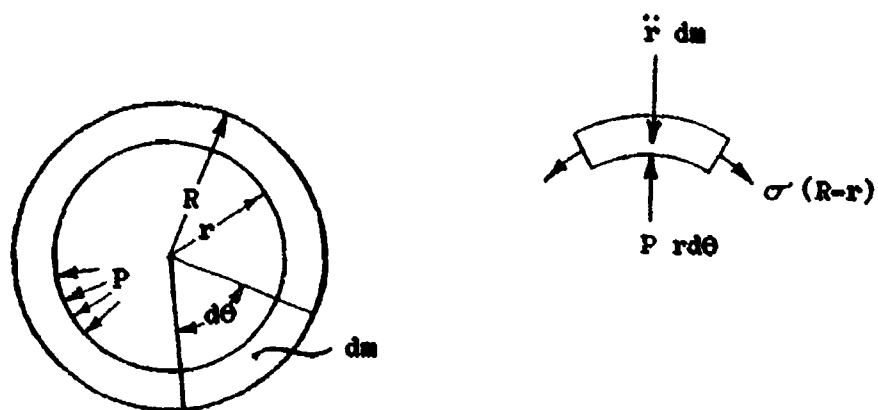


Figure 1. Diagram for the Determination of the Radial Motion Equation.

Since plastic deformation is a constant volume process, a constant volume expansion is assumed. Therefore, for a unit length of cylinder the following relation will hold:

$$\begin{aligned}
 A_0 &= \pi (R_0^2 - r_0^2) = \pi (R^2 - r^2) = \pi (R-r)(R+r) \\
 (R-r) &= \frac{(R_0^2 - r_0^2)}{(R+r)} = \frac{(R_0^2 - r_0^2)}{(R-r) + 2r} \\
 (R-r)^2 + (R-r)(2r) - (R_0^2 - r_0^2) &= 0 \\
 (R-r) &= -r \pm \sqrt{r^2 + R_0^2 - r_0^2} = -r + \sqrt{(r^2 - r_0^2) + R_0^2} \\
 \therefore \dot{r} &= \frac{2Pr - 2\sigma [-r + \sqrt{r^2 + (R_0^2 - r_0^2)}]}{\rho (R_0^2 - r_0^2)} \quad (4)
 \end{aligned}$$

Assuming an isentropic expansion,

$$\begin{aligned}
 Pv^\gamma &= \text{constant} \\
 P &= P_0 \left(\frac{v_0}{v} \right)^\gamma = P_0 \left(\frac{r_0}{r} \right)^{2\gamma}
 \end{aligned}$$

for a circular cross-section of unit length. Therefore, Equation (4) becomes:

$$\dot{r} = \frac{2P_0 r_0^{2\gamma}}{\rho (R_0^2 - r_0^2)} r^{-(2\gamma-1)} + \frac{2\sigma}{\rho (R_0^2 - r_0^2)} \left[r - \sqrt{r^2 + (R_0^2 - r_0^2)} \right]$$

To simplify the notation, let

$$A = \frac{2P_0 r_0^{2\gamma}}{\rho (R_0^2 - r_0^2)}, \quad B = \frac{2\sigma}{\rho (R_0^2 - r_0^2)}$$

$$\text{then } \dot{r} = Ar^{-(2\gamma-1)} + B \left[r - \sqrt{r^2 + R_0^2 - r_0^2} \right]$$

$$\dot{r} = \frac{dV}{dt} = \frac{dV}{dr} \frac{dr}{dt} = V \frac{dV}{dr}$$

$$2VdV = 2 \left[A r^{-(2\gamma-1)} + Br - B(r^2 + R_0^2 - r_0^2)^{\frac{1}{2}} \right] dr$$

$$V^2 = -\frac{A}{\gamma-1} r^{-(2\gamma-2)} + Br^2 - B \left[r\sqrt{r^2 + R_0^2 - r_0^2} + (R_0^2 - r_0^2) \ln (r + \sqrt{r^2 + R_0^2 - r_0^2}) \right] + C_1$$

or extracting part of the arbitrary constant, C_1 , to make the logarithm dimensionless,

$$V^2 = B \left[r^2 - r\sqrt{r^2 + R_0^2 - r_0^2} - (R_0^2 - r_0^2) \ln \left(\frac{r + \sqrt{r^2 + R_0^2 - r_0^2}}{\sqrt{R_0^2 - r_0^2}} \right) \right] - \frac{A}{\gamma-1} r^{-(2\gamma-2)} + C$$

to evaluate C , the above is solved for C assuming $V = V_0$ at $r = r_0$ and

$$C = V_0^2 + \frac{2}{\rho} \left[\frac{r_0 \sigma}{R_0 + r_0} + \frac{\sigma}{2} \ln \left(\frac{R_0 + r_0}{R_0 - r_0} \right) + \frac{P_0 r_0^2}{(R_0^2 - r_0^2)(\gamma-1)} \right]$$

The equation for V^2 will be rearranged by introducing the following quantities.

$$F = \frac{1 - \left(\frac{r_0}{r}\right)^{2(\gamma-1)}}{\gamma-1}, \text{ dependent upon } r \text{ and } \gamma$$

$$G = r^2 - r\sqrt{r^2 + R_0^2 - r_0^2} - (R_0^2 - r_0^2) \ln \left(\frac{r + \sqrt{r^2 + R_0^2 - r_0^2}}{\sqrt{R_0^2 - r_0^2}} \right)$$

$K = \frac{2 P_0 r_0^2}{\rho(R_0^2 - r_0^2)}$, a constant for a given set of initial conditions.

$L = \frac{2}{\rho} \left[\frac{r_0 \sigma}{R_0 + r_0} + \frac{\sigma}{2} \ln \frac{R_0 + r_0}{R_0 - r_0} \right]$, a constant for a given set of initial conditions.

$B = \frac{2\sigma}{\rho(R_0^2 - r_0^2)}$, defined previously, dependent upon σ .

Using these values, $V^2 = KF + BG + L + V_0^2$ (5)

the quantity $BG + L$ is zero at $r = r_0$ and except for very large $\frac{r}{r_0}$ (>3) or thick cylinders (wall thickness $\geq r_0$) or σ greater than $.1 P_0$, this will be negligible compared to KF . If P_0 is assumed to be of the order of 10^8 lbs. per square foot, and σ of the order of 10^7 lbs. per square foot, the only terms contributing to the calculation of V^2 will be

KF and V_0^2 . Since the final value of V is of the order of several thousand feet per second and the order of V_0 is of the order of several hundred feet per second, V_0 will be neglected for the initial analysis. Thus Equation (5) may be simplified to

$$\begin{aligned} V^2 &= KF \\ V &= \sqrt{KF} \end{aligned} \tag{5a}$$

The resulting equation for V can be integrated exactly only for certain values of γ . In general a numerical integration process is required to obtain the required curves of r vs. t and V vs. t . To accomplish this, assume the following test conditions.

$$\begin{aligned} P_0 &= 1 \times 10^8 \text{ psf} \\ \rho &= 15.25 \text{ slugs/ft}^3 \text{ (steel)} \\ R_0 &= .1667 \text{ ft} \\ r_0 &= .125 \text{ ft} \\ \gamma &= 3.0 \\ V_0 &= 0 \end{aligned}$$

Then V is plotted as a function of $\frac{r}{r_0}$, Figure 2, $\frac{1}{V} = \frac{dt}{dr}$ is plotted as a function of $\frac{r}{r_0}$, and the latter curve is integrated graphically to obtain a plot of $\frac{r}{r_0}$ vs. t , Figure 3. By cross referencing Figures 2 and 3, a plot of V vs. t is obtained, Figure 4. Figures 3 and 4 are then used in conjunction with the calculated values of time as a function of position of the detonation wave in the cylinder to determine shape and velocity profile of the casing. Representative curves showing velocity as a function of position along the cylinder, x , for four different times during the expansion process in a center detonated cylinder are shown in Figure 5.

The direction of the velocity vector for a given fragment will be obtained from the shape of the casing at the time of break-up (Section B) and will be approximated by the Taylor Angle, i. e., one half the angle formed by the normal to the cylinder axis and the normal to the surface of the expanded cylinder in the region of interest.

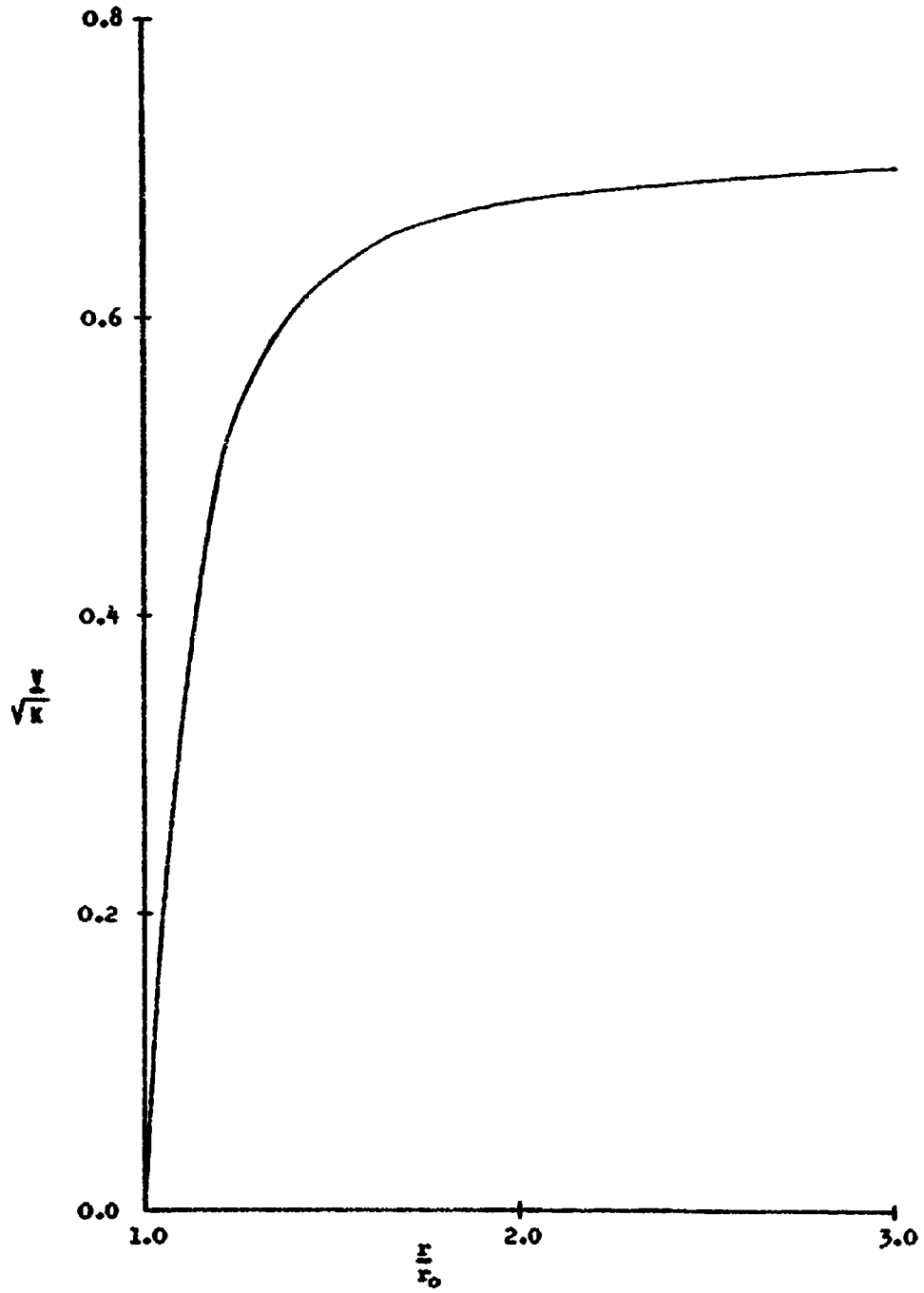


Figure 2. Velocity Versus Radius of the Cylinder in Terms of Dimensionless Variables.

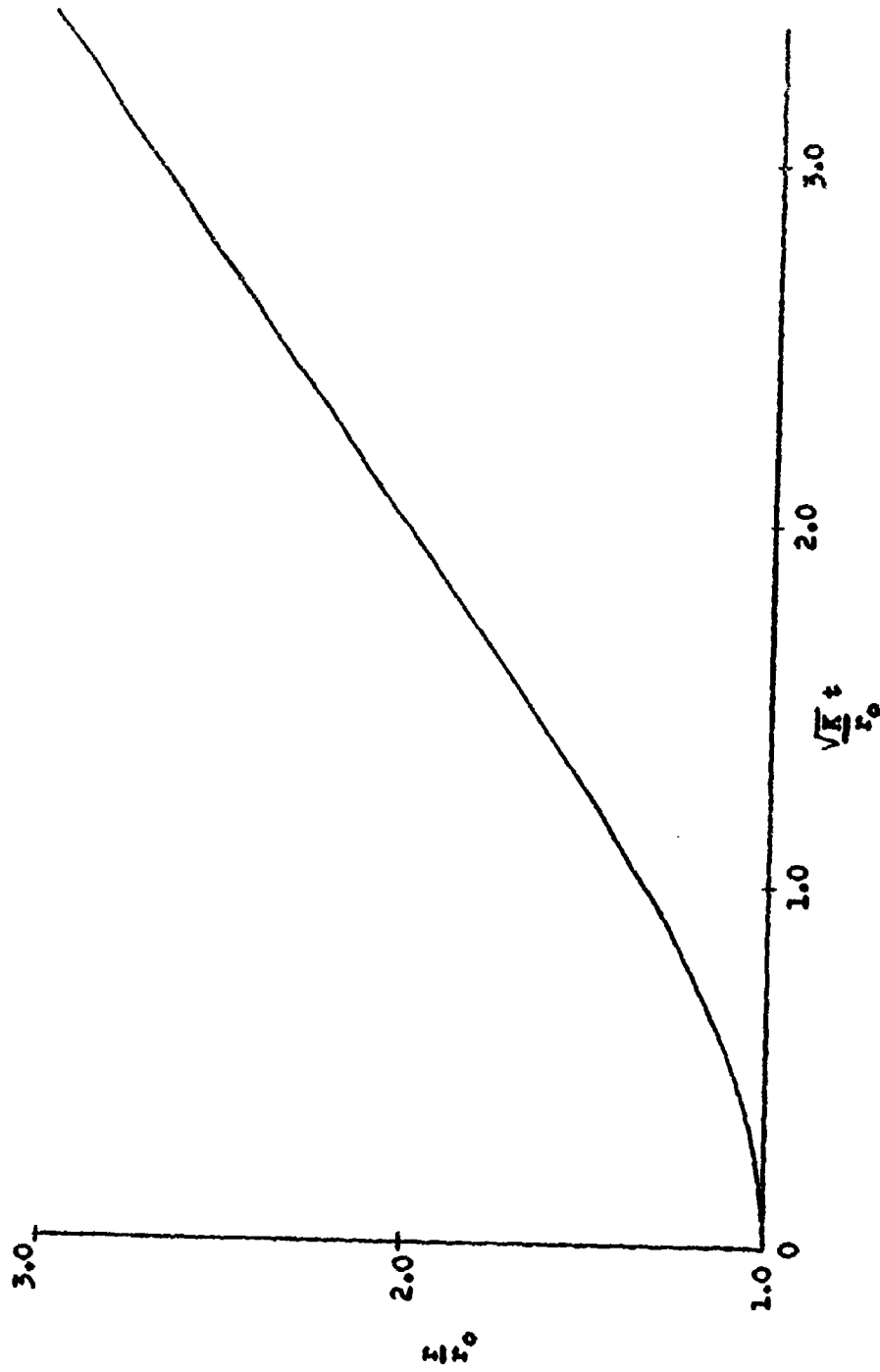


Figure 3. Radius of the Cylinder Versus Time in Terms of Dimensionless Variables.

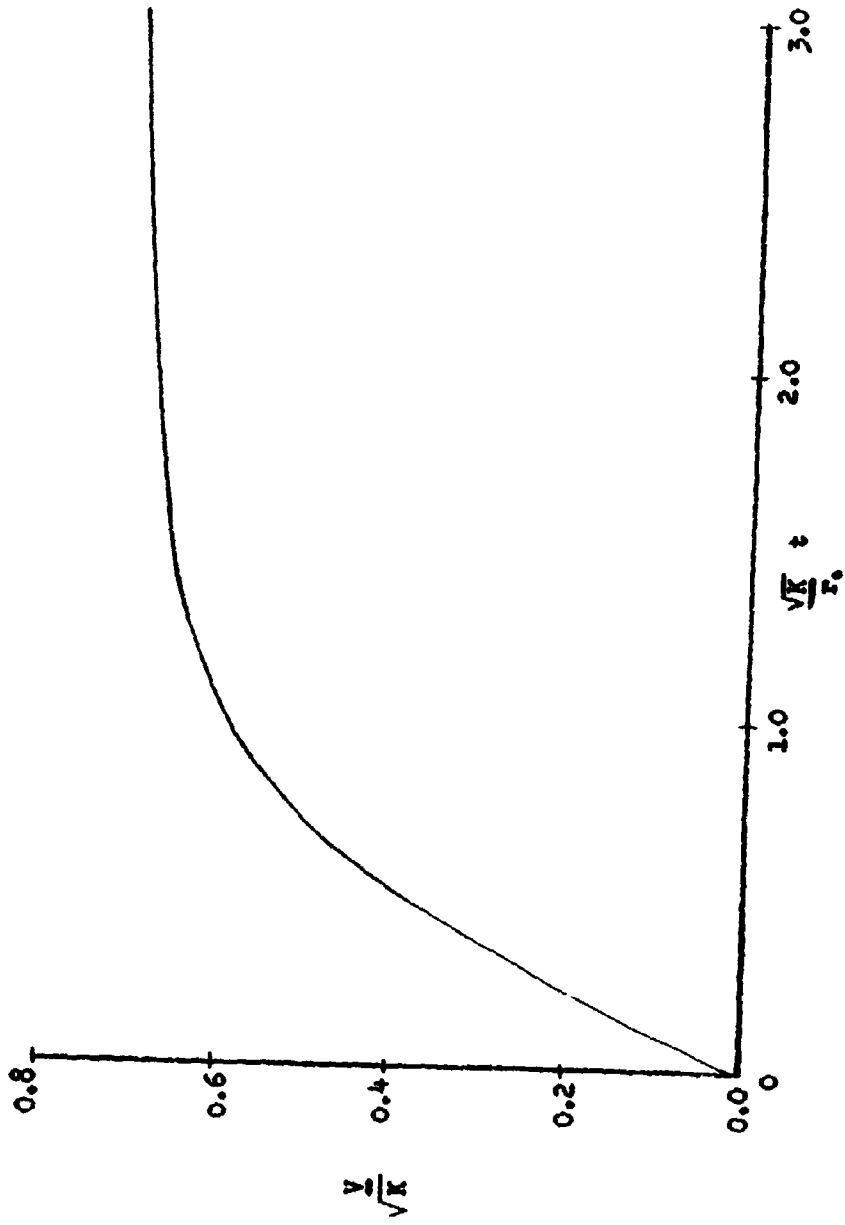


Figure 4. Velocity of the Cylinder Wall Versus Time in Terms of Dimensionless Variables.

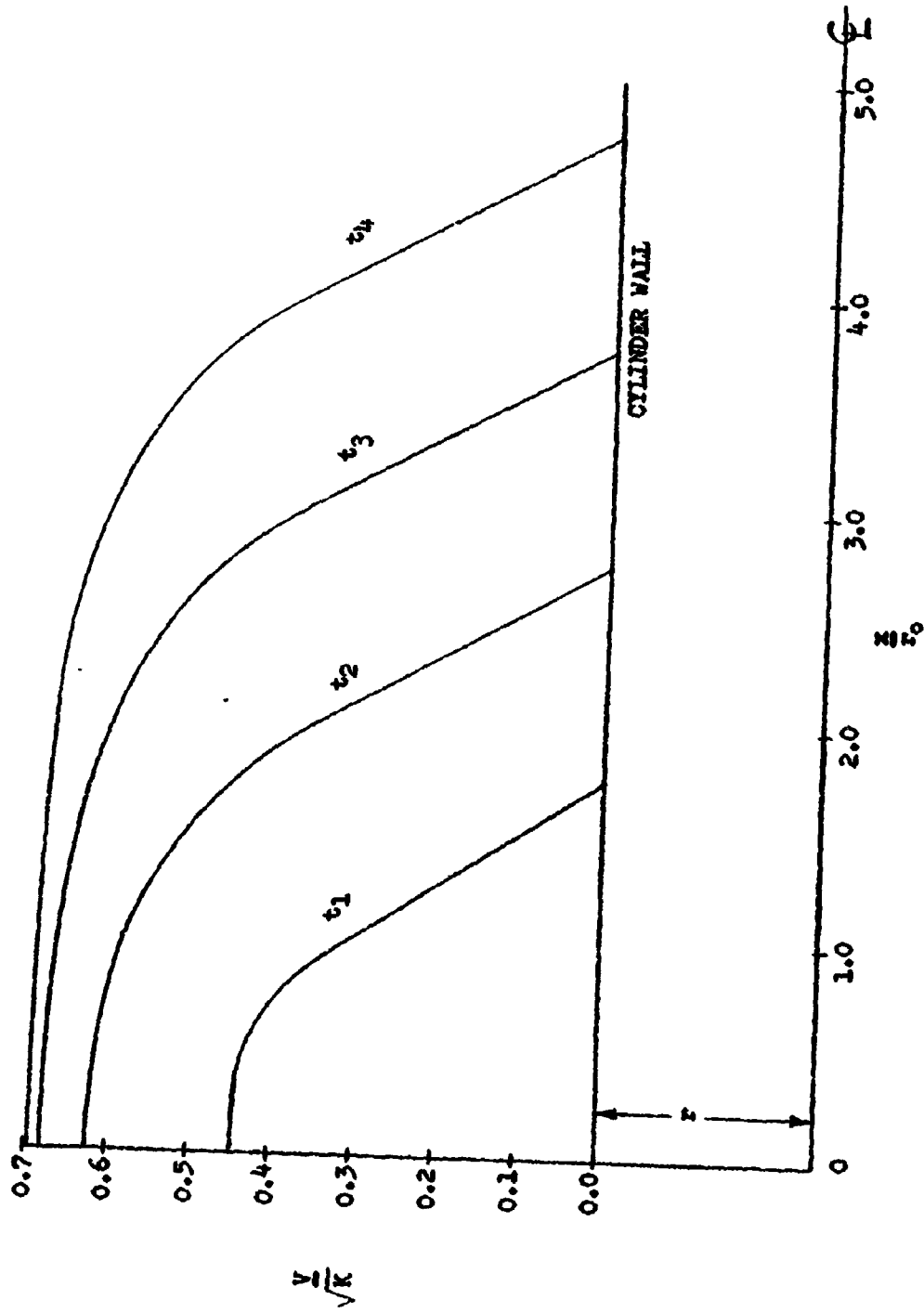


Figure 5. Velocity of the Cylinder Wall at Various Positions Along the Cylinder for Four Different Time Increments.

To examine the effect of various values of γ on the velocity of an expanding cylindrical casing assume that $V_0 = 0$ and that σ is negligible. The assumption regarding σ will not affect the results more than 5% for initial pressures greater than 1×10^8 psf. With these assumptions, Equation (5) reduces to Equation (5a) as before, i. e.:

$$V^2 = \frac{2 P_0}{\rho(R_0^2 - r_0^2)(\gamma - 1)} \left[r_0^2 - r_0^{2\gamma} r^{-(2\gamma-2)} \right]$$

$$V^2 = \frac{2 P_0 r_0^2}{\rho(R_0^2 - r_0^2)} \frac{1 - \left(\frac{r_0}{r}\right)^{2\gamma-2}}{\gamma-1} = K \frac{1 - \left(\frac{r_0}{r}\right)^{2(\gamma-1)}}{\gamma-1} = KF$$

where K is a constant dependent upon the initial internal and external radii of the cylinder and the initial pressure of the explosive, and F is a function of γ . From this we see that velocity is a function of \sqrt{F} . Plotting \sqrt{F} vs. $\frac{r_0}{r}$ for various values of γ , Figure 6, we find that for r close to r_0 , that is, early in the expansion process, the value of γ is relatively unimportant. In fact at $r = r_0$, the slope of the curve is determined by

$$\frac{\partial F}{\partial r} \Big|_{r=r_0} = \frac{1}{\gamma-1} \left[-2(\gamma-1) \left(\frac{r_0}{r}\right)^{2\gamma-3} \left(-\frac{r_0}{r^2}\right) \right] \Big|_{r=r_0} = \frac{2}{r_0}$$

which is independent of γ . Presumably, γ can be quite high (5 or higher) early in the expansion process, but drops rapidly due to the decrease in pressure. Therefore, once a value of γ has been determined which defines the expansion process at the point of maximum expansion, the assumption that this value remains constant for the entire expansion process should present no serious errors in the velocity determination.

The dependence of the velocity of the expanding casing upon the pressure developed by the explosive used is presented in Figure 7. It may be observed that the shape of the two curves are the same. However, with a threefold decrease in pressure the lower curve is displaced by a constant factor of $\frac{1}{\sqrt{3}}$ from the upper curve. This significant influence on velocity points out the relative importance of the type of explosive used, and the necessity of selecting the proper explosive to attain the desired fragment velocity.

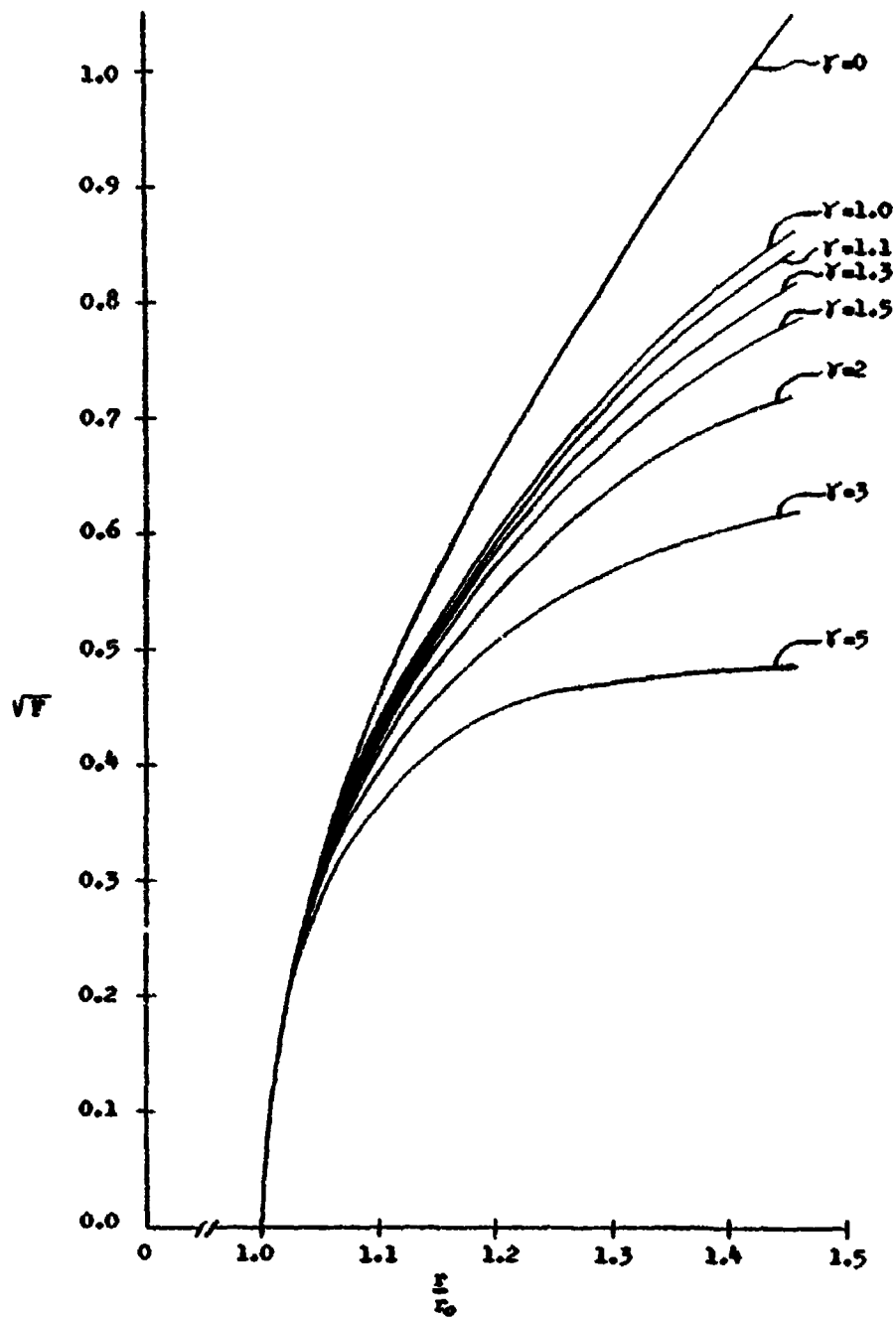


Figure 6. Variation of the \sqrt{F} (Proportional to Velocity) Versus Radius of Cylinder for Various Values of the Specific Heat Ratio (γ).

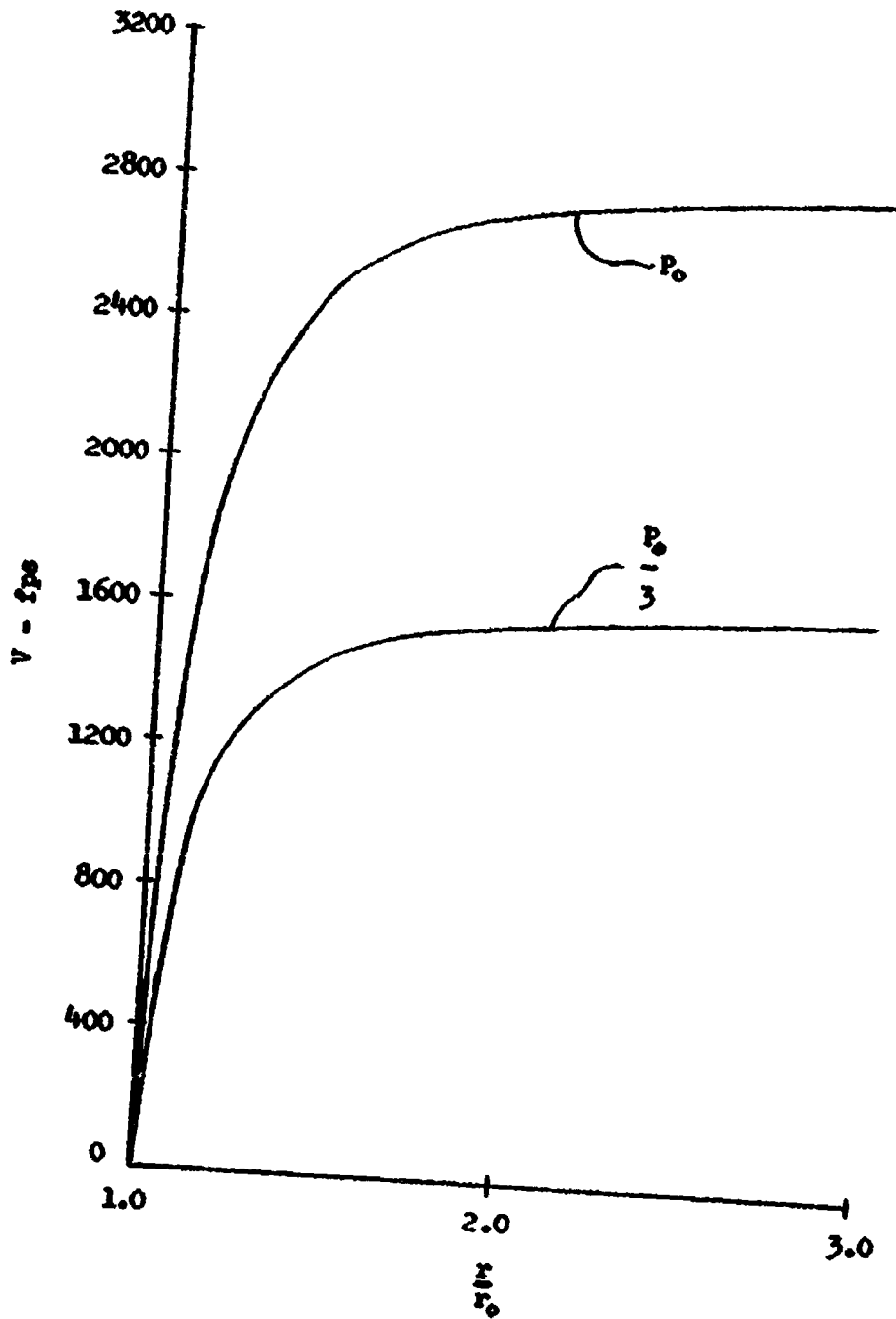


Figure 7. Variation of Velocity Versus Radius of the Cylinder as a Function of the Initial Pressure.

I. Determination of the Shape of Casing During Expansion

In this program it will be assumed (1) that a knowledge of the shape of the casing during the detonation process will be sufficient to determine the average direction of fragment travel from a given point on the casing, (2) that the rate of change of the casing motion (velocity) at the time of breakup will be the initial velocity of the fragment, and (3) that the size and number of fragments may be determined from a statistical analysis using probability of fracture as a function of strain and time.

An accurate determination of the shape of exploding cylinders and plates should include a real equation of state for both the gaseous explosion products and the metal casing, and multi-dimensional flow equations for the gas. However, since accurate equations of state for gases under the conditions prevailing in a detonation process are not generally known, and multi-dimensional flow equations are quite difficult to solve without recourse to high speed computer techniques, such an accurate determination of shape during the expansion process could become extremely involved. Investigators in the field have made numerous attempts at simplifying the problem. Computer programs have been developed to account for the multi-dimensional gas flow. (See Appendix A.) One of these, the Cyclone Code, assumes a perfect gas expansion with ratio of specific heats, γ , approximately equal to 3 (2.6 to 2.8 for various explosives). Another program, the Roc code (Pierson at Picatinny) makes use of more sophisticated equations of state in the gas and in the casing.

The analysis presented below provides a simplified method for determining the shape of the casing at any time during the expansion process.

The initial assumption will be the same as that made by Gurney and G. I. Taylor, i. e., that the pressure over a given cross section in a center detonated cylinder varies with time but is uniform over the section. It will be further assumed, for a first approximation, that there is no axial gas flow during the expansion process. End effects will be neglected for the present and the model will consist of a long cylinder, filled with explosive, detonated on the axis at a point midway between the ends of the cylinder. It will be assumed for purposes of determining shape that the casing has mass but no strength in tension or shear. The sequence of events during the expansion process is then explained as follows. (See Figure 8.)

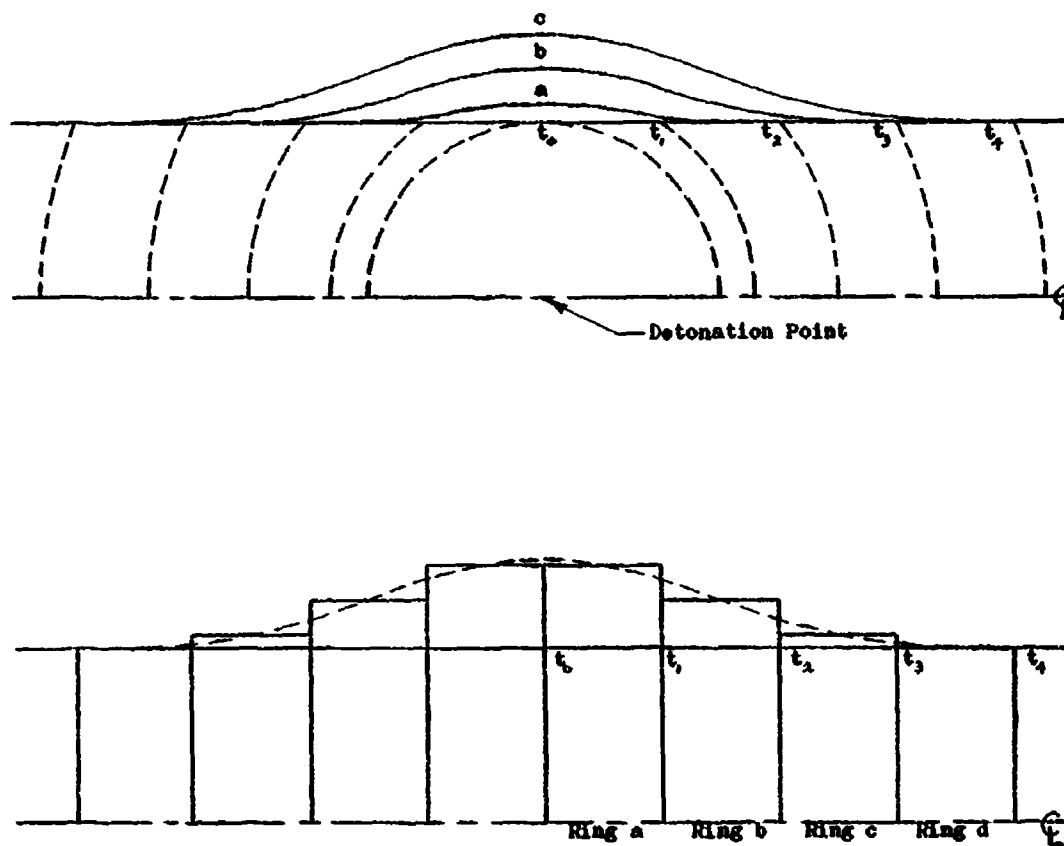


Figure 8. Determination of Cylinder Shape as a Function of Time.

It is assumed that the casing material moves radially as a series of independent rings under the influence of the gas contained within the rings. No motion takes place until the detonation front reaches position 1 in Figure 8. At this time, t_1 , the first or center segment begins to move under the influence of the gas contained within it. The next segment on either side of the center does not begin to move, however, until the detonation front reaches position 2. At this time, t_2 , the first segment has moved to curve a and the casing then appears approximately as shown by curve a. The process then continues as the detonation front progresses along the surface of the cylinder. To obtain the deflection curves of the cylinder, requires the expansion of the individual segments as a function of time, and the time of arrival of the detonation front at any point along the cylinder.

To determine the time of arrival of the detonation front, consider Figure 9. Assume a detonation velocity, c , and a distance along the cylinder from the point of initiation to the point of contact of the detonation wave with the cylinder wall, x . The radius of the detonation front is a , and the initial radius of the cylinder is r_0 . Then:

$$a = c t$$

$$r_0^2 + x^2 = a^2 = c^2 t^2$$

$$t = \frac{1}{c} \sqrt{r_0^2 + x^2} = \frac{r_0}{c} \sqrt{1 + \frac{x^2}{r_0^2}}$$

This expression will then provide values of time, t_1 , t_2 , t_3 , t_4 , at which the detonation front arrives at points 1, 2, 3, and 4 respectively, in Figure 8. With the detonation front at point 4, for example, the total time of expansion of ring c will be $t_4 - t_3$, that of ring b will be $t_4 - t_2$, and that of ring a will be $t_4 - t_1$. Plotting the radii of the various rings using Figure 3 then provides a shape determination at any time, t , determined by the location of the detonation front at that time. (See Figure 10.)

It is to be noted that the same expansion characteristics are assumed for each segment of the casing and the shape is derived from the variable time of application of pressure from the detonation wave. Thus, irregular shapes may be analyzed by changing the expansion characteristics of the gas and the time of application of the detonation pressure over various elements of the casing. Modifications of the expansion process may also be used to analyze buffers and unusual explosive configurations.

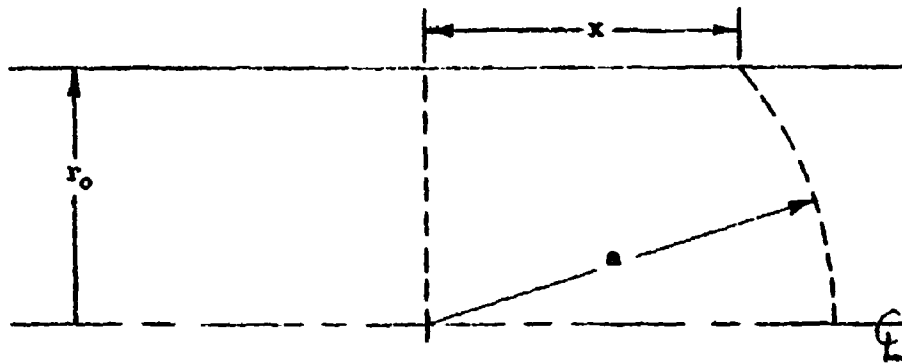


Figure 9. Schematic for Determination of the Time of Arrival of the Detonation Front at the Cylinder Wall.

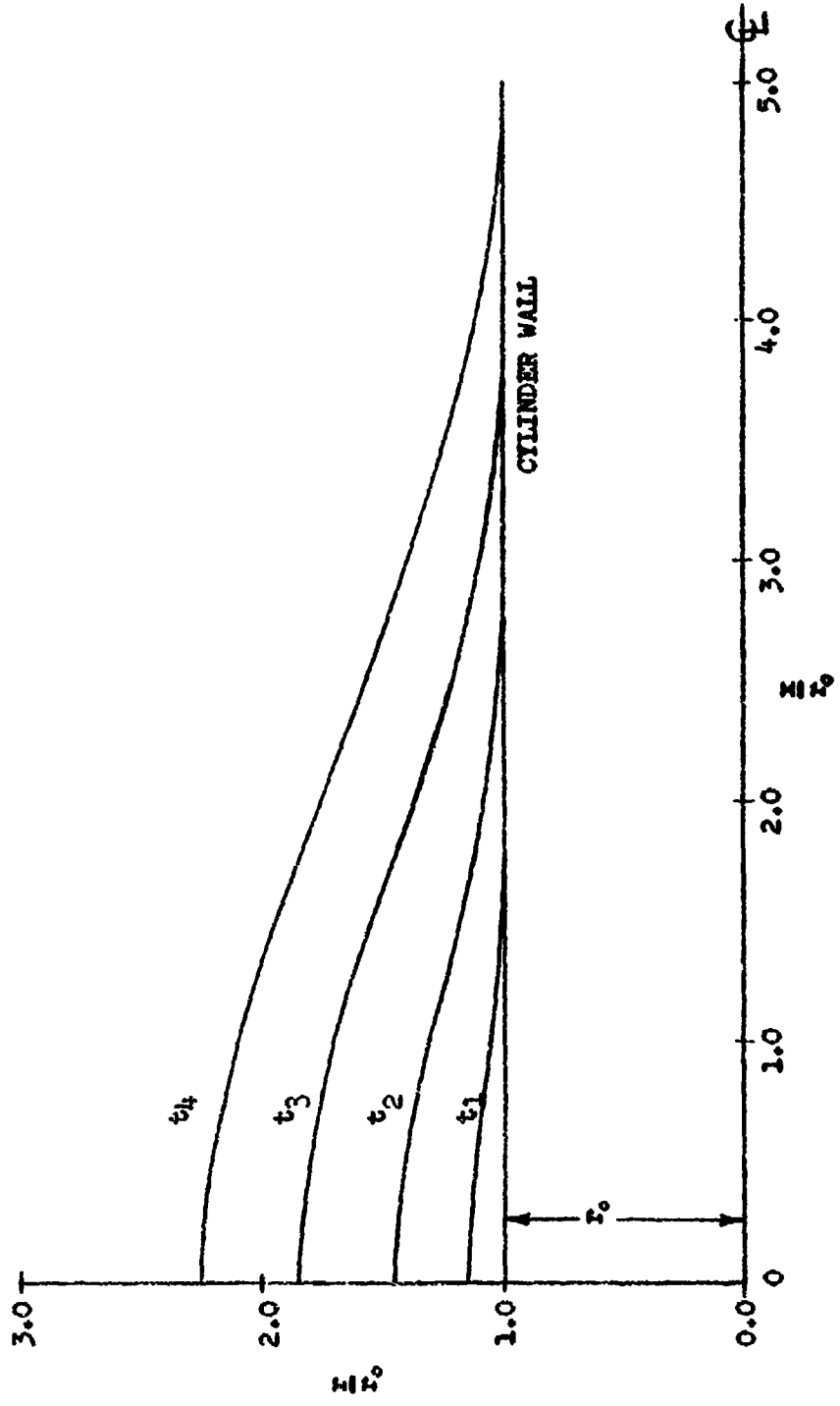


Figure 10. Radius of the Cylinder at Various Positions Along the Cylinder Wall for Four Different Time Intervals.

C. Determination of Fragment Distribution and Size

The approach used in this program for describing the explosive breakup of metal cylinders, plates or spheres is based upon probability considerations and is similar in part to that proposed by N. F. Mott.¹ The total problem of breakup is not encountered in Mott's treatment since only circumferential strains are considered. It is obvious that to fully describe the breakup of a continuous cylinder, both circumferential and longitudinal strains must be considered.

1. Determination of Strain

The statistical method of determining breakup, which will be explained later, requires the determination of the conditions of strain at any point on the cylinder as a function of time. For purposes of analysis the strain will be assumed to consist of two independent components. One of these, the circumferential strain, is directly proportional to the radial displacement of a given ring, and may, therefore, be determined directly from the position-time curves described previously. The other component, the longitudinal strain, is somewhat more difficult to obtain. The determination of longitudinal strain which will be used in future analyses is explained by the following.

It will be assumed that the shape of the casing during the detonation process is given by the analysis described previously in Section B. As the casing expands, the particles will travel paths corresponding to the assumed direction of the velocity vector, i. e., the particles will start radially and thereafter follow paths determined by the "Taylor angle" (defined on page 16) measured at the corresponding points on the expanded surface of the casing. Thus, the particles directly over the initiation point will continue to move radially while all other points will follow paths curving away from a plane perpendicular to the axis of the cylinder passing through the initiation point. (Figure 11.) This will provide a maximum longitudinal strain and strain rate immediately over the initiation point with strain decreasing to a nearly constant value along the axis as the path lines become nearly parallel. This condition will tend to promote small, nearly rectangular fragments near the initiation point where the circumferential and longitudinal strains are nearly equal, and longer fragments farther along the cylinder where the longitudinal strain is less than the circumferential strain.

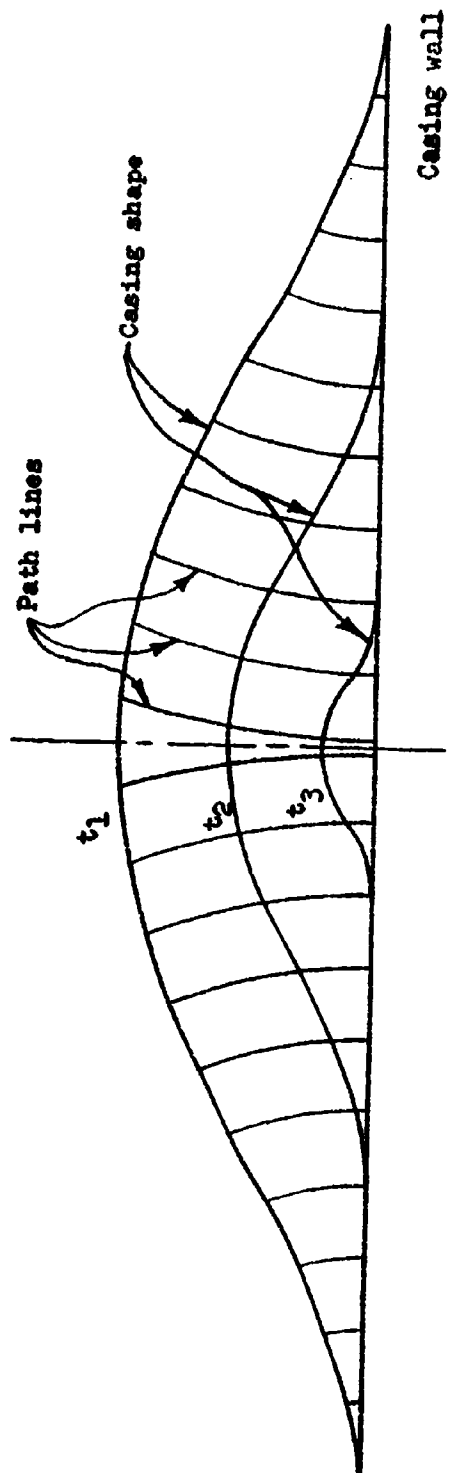


Figure 11. Path of Particles Within the Casing Wall as a Function of Time.

2. Application of Statistics to the Method of Breakup

The following analysis is due in part to Mott. In his analysis, Mott predicts the breakup of a ring wherein each fracture is assumed to occur over the entire cross section of the ring simultaneously, thus breaking the ring. A release wave then propagates through the ring away from the fracture, and at some later time a second fracture occurs in some part of the ring not yet reached by the release wave. A second pair of release waves then emanate from the second fracture and the process is repeated until the release waves join to relieve all stress in the ring. At this time the fragmentation process is complete.

Attempts will be made to apply a similar but expanded method to the breakup of a center detonated cylinder with the following modifications.

a. The fracture will be assumed to occur instantaneously through the cross section of a region of constant stress and will propagate at a velocity determined by the properties of the casing material.

b. It will be assumed that a stress relief wave propagates in a direction perpendicular to the fracture at a constant velocity determined by the properties of the casing material.

c. Both circumferential and longitudinal strains will be considered in the final statistical analysis.

To clarify the process, a review of the method proposed by Mott is as follows. Define the strain in terms of the original circumference of the casing material, l_0 , and the final circumference l , as

$$s = \frac{l - l_0}{l_0} = \frac{l}{l_0} - 1$$

Now assume that the chance that a specimen of unit length not yet fractured will fracture when the strain increases from s to $s + ds$ is

$$C e^{as} ds$$

Then the probability, dp , that any specimen will fracture between s and $s + ds$ will be the product of the above expression and the probability that the specimen reached a strain value s without fracturing. If p

is the probability that the specimen breaks before a strain s is reached, then we have

$$dp = (1-p) C e^{as} ds$$

and upon integrating both sides,

$$\int_0^p \frac{dp}{1-p} = \int_0^s C e^{as} ds$$

$$- \ln(1-p) = \frac{C}{a} e^{as}$$

$$p = 1 - \exp - \left(\frac{C}{a} e^{as} \right)$$

The probability of fracture as a function of strain is shown in Figure 12. The strain, here assumed to be 0.5, is the strain at which the probability of fracture is 0.5. Assuming a constant rate of strain increase, it is seen that the probability of fracture will increase from a low value to a value near one as the strain passes through a range around the average strain. The width of this range is determined by the value of a used for the casing material. A value of $a = 50$ was used to plot the curve shown. In general, a lower value of a widens the range and a higher value makes the range narrower. Thus, the higher a values correspond to shorter times for the probability of strain to increase from a low value to near unity with a given strain rate. Since the fragment size will depend upon the length of time between fractures (time during which stress relief waves may travel) the higher values of a suggest a greater number of smaller fragments, conversely, a lower value of a suggests fewer but larger fragments. Now, the average strain for fracture is given by

$$s_0 = \int_{-\infty}^{\infty} s \frac{dp}{ds} ds = \int_{-\infty}^{\infty} s \exp - \left(\frac{C}{a} e^{as} \right) C e^{as} ds$$

$$s_0 = \frac{1}{a} \left[\ln \frac{a}{C} + \epsilon \right]$$

$$\epsilon = \int_0^{\infty} \ln x e^{-x} dx = -0.577 \dots$$

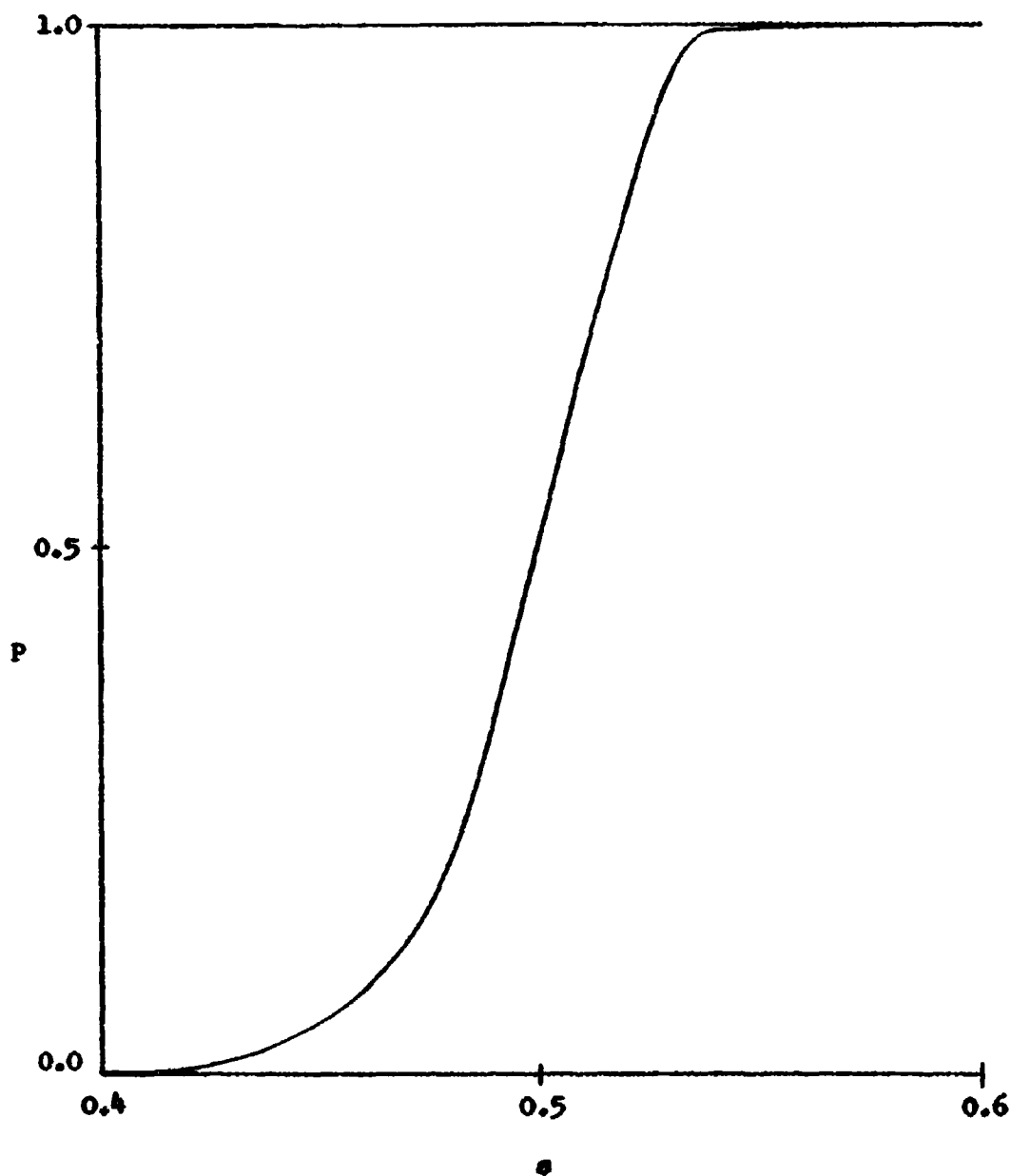


Figure 12. Probability of Fracture as a Function of Strain.

and the r. m. s. of the scatter in the strains at fracture is

$$\left\{ \int_0^{\infty} (s-s_0)^2 \frac{dp}{ds} ds \right\}^{\frac{1}{2}} \approx \frac{1.28}{a}$$

thus for a a (dependent upon material properties) of 128, the rms of the scatter in strains is 0.01.

At this point, the Mott analysis is modified somewhat by the assumption of constant relief wave velocity. The breakup of a ring by fractures in the axial direction will be considered first. If the length of the unfractured ring is $l = 2\pi r$, and at some time, t , n fractures have occurred, then the rate of increase of fractures is given by

$$\frac{dn}{ds} = lfC e^{as}$$

where f is the proportion of the ring still unstressed. Introducing the variable

$$\phi = as, \text{ then}$$

$$\frac{dn}{d\phi} = \frac{lfC}{a} e^{\phi} \quad (6)$$

If the stress relieved region around a crack propagates into the material with velocity V_s and the strain rate is assumed constant during the fracture process,

$$\frac{ds}{dt} = \frac{V}{r}$$

where V is the velocity of the ring and r the radius, then

$$s = \frac{V}{r} t$$

$$\phi = a \frac{V}{r} t$$

Thus, ϕ is proportional to time as the fracture process progresses. If a fracture occurs at $\phi = \phi_p$, the region about the fracture which is stress relieved, and hence safe from further fracture at any later time, is then

$$\begin{aligned}
 x &= V_s (t-t_1) \\
 &= V_s \frac{\phi r}{a V} - \frac{\phi_1 r}{a V} \\
 &= V_s \frac{r}{a V} (\phi - \phi_1) \\
 &= x_0 (\phi - \phi_1)
 \end{aligned}$$

where $x_0 = V_s \frac{r}{a V}$

Prior to the first fracture, Equation (6) can be integrated treating f as constant and equal to 1. Thus, at the time the first fracture occurs, $n = 1$ and from (6)

$$1 = \frac{l C}{a} e^{\phi_0}$$

where ϕ_0 is defined as that value of ϕ corresponding to the time, t_0 , at which the first fracture occurs.

$$\phi_0 = \ln \frac{a}{l C}$$

and (6) may be written as

$$dn = f e^{(\phi - \phi_0)} d\phi$$

An analytical expression for f can be obtained as follows. Consider the time after the first fracture, but prior to the second fracture in a ring. During this time, a stress relief wave travels through the ring at velocity V_s from both sides of the fracture. The fraction of the ring still stressed at any time t is then

$$f = \frac{l - 2V_s(t-t_0)}{l} = 1 - \frac{2V_s}{l} (t-t_0)$$

If the second fracture occurs at time t_1 , then from that time on, two additional relief waves propagate through the ring and the fraction of the total ring still stressed is

$$f = 1 - \frac{2V_s}{l} (t-t_0) - \frac{2V_s}{l} (t-t_1)$$

The general expression for f at any time, provided that none of the relief waves meet in the ring, is

$$f = 1 - \frac{2 V_s}{l} \left[Nt - \sum_{k=0}^{N-1} t_k \right] \quad (7)$$

Where N is the number of longitudinal fractures that have occurred and t_k are the times at which the fractures occurred. If two relief waves intersect at time t_p , then at this time the rate of propagation of stress relief will be reduced by $2 V_s$. If P is defined as the number of such intersections and t_p the time at which they occurred, then (7) becomes

$$f = 1 - \frac{2 V_s}{l} \left[(N-P)t - \sum_{k=0}^{N-1} t_k + \sum_{p=0}^P t_p \right] \quad (8)$$

substituting (8) into (6) and integrating, it can be shown that

$$n = 1 + \left\{ \exp \left[\frac{a V}{r} (t-t_0) \right] - 1 \right\} \left\{ f + \frac{2 V_s r (N-P)}{l a V} \right\} - \frac{2 V_s}{l} (N-P)(t-t_0) \quad (9)$$

Equation (8) and, hence, (9), is discontinuous and cannot be solved directly for t . However, graphical techniques similar to those used by Mott can be used here to determine the total number of fragments and the fragment distribution due to circumferential strains.

The method for determining the longitudinal strain along a cylinder was discussed previously in the section on the determination of strain. Although the methods for determining longitudinal strain appear very feasible at this time; no actual statistical approach has been derived which accounts for all of the variables of the system. Because of this no complete mathematical model has been developed to date.

3. Method of Breakup

A method has been presented by which certain predictions as to fragment size and distribution can be made in the case of a uniformly stressed ring having a given rate of increase of strain. This method will now be qualitatively extended to apply to breakup over an area. It will be assumed that a given area of casing material is uniformly stressed in tension in all directions. This condition is closely

approximated by a small portion of an exploding sphere. The breakup process is shown schematically in Figure 13. In order to simplify the process, it is assumed that the first cracks formed are at right angles, and during the breakup all succeeding cracks are parallel or perpendicular to the original cracks. Early in the fragmentation process, the cracks may actually start in random directions. However, as a given crack progresses through the material, the stress is relieved on either side in a direction such that the only stress left in the material tends to promote additional cracks perpendicular to the first crack. In any geometry other than spherical, it is probable that the stress will build up initially in a preferred direction, thus, promoting formation of the early cracks perpendicular to the direction of highest stress. Thus, the model chosen for illustration in Figure 13 is a square which has been subdivided into ten horizontal and ten vertical bands. It is assumed that all cracks formed will be either horizontal or vertical.

General rules have been followed in constructing the simulated breakup shown. These are as follows:

- a. When a crack initiates, it forms simultaneously over the narrow dimension of a band and begins to propagate at some velocity into the neighboring bands. Cracks form only at the edges of bands.
- b. When a crack is formed in a band, a release wave propagates along the band perpendicular to the crack, and moves along the band away from the crack in both directions.
- c. If a crack forms at a point in a band closer than one band width to a point in an adjacent band where a crack has previously started, then the new crack becomes an extension of the old crack. Thus, the apparent velocity of crack propagation can be much higher than that normally assumed.
- d. If a crack propagates into a previously formed crack at right angles it is stopped.
- e. If a crack propagates into a region in which stress has been relieved from a previous parallel crack, it is stopped.
- f. When the entire surface has been relieved of stress in both directions, the fragmentation process is complete.

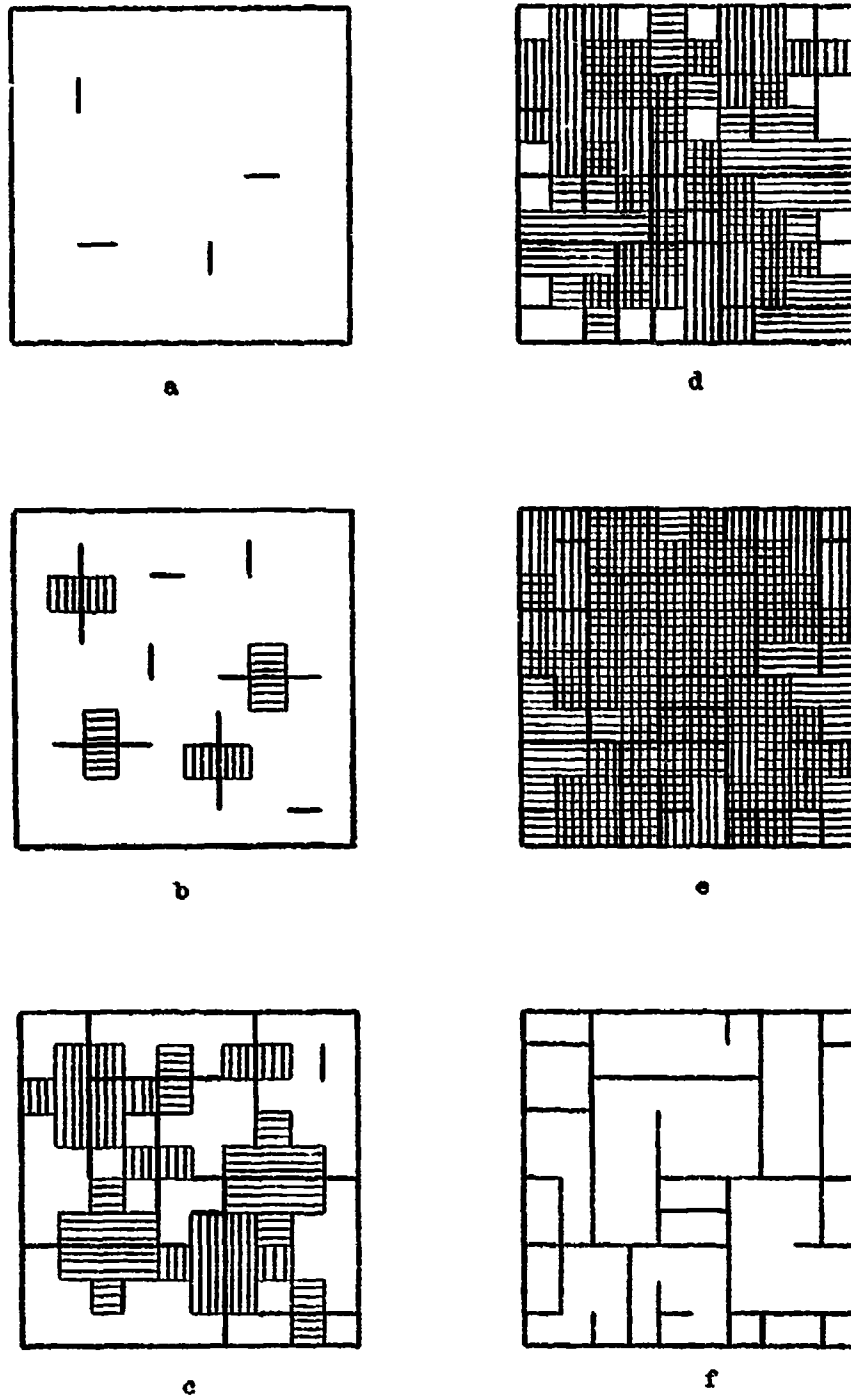


Figure 13. Schematic of Fragmentation Process for a Uniformly Stressed Section.

The process depicted in Figure 13 is as follows. At a, four initial cracks have started. These were selected at random, rather than assuming a given strain rate and attempting to apply strict statistical methods. At b, the four original cracks have grown to three times their original length, cracks having formed on either end of the original cracks in adjacent bands. A stress relief wave has propagated on either side of the four original cracks, and four new cracks have formed.

At c, the original cracks have propagated across new bands and the stress relief waves have continued to propagate away from earlier cracks. Again, several new cracks have formed. At d, some cracks have been stopped by other cracks or by stress relieved regions, and most of the plate has been stress relieved in one direction or the other. At e, the last of the new cracks have formed and the fragmentation process is nearly complete.

The shaded areas in b through e represent regions of stress relief. At f, the entire plate is stress relieved and the fragmentation process is complete. Note the frequent occurrence of cracks which have propagated into a fragment, but not entirely through it. Such "split" fragments are often observed. The model shown in Figure 13 is meant for illustrative purposes only. No attempt has been made at this time to rigorously plot a fragmentation process.

The problem at hand, i. e., that of an exploding cylinder or a nonuniformly exploding plate, presents some additional problems. Aside from the time element introduced into the process by the Mott analysis, there is an additional time element in an actual detonation. This additional time element is caused by the rate of application of force to the casing which in turn is dependent upon geometry and explosive characteristics. These time elements must be combined statistically to provide a realistic determination of the fragmentation process. Investigation of these effects plus further development of the statistical approach for defining fragmentation by a probability technique based upon strain criteria will constitute the major effort for the next reporting period.

APPENDICES

APPENDIX A

THE GURNEY EQUATION

The development of Gurney type equations will be discussed since some of the assumptions used by Gurney and others have been analyzed in this study. The Gurney formula will be derived for three cases: (A) the one dimensional, or "piston" type of expansion, (B) the two dimensional, or cylindrical expansion, and (C) the three dimensional or spherical expansion. The following general assumptions are made:

1. The detonation front reaches all points of the casing simultaneously, and, thereafter, the pressure within the casing varies with time but not with linear dimension. Thus, at any given time, the pressure within the casing will be the same everywhere.

2. The strength of the casing wall is negligible, and all fragments are ejected simultaneously.

3. The final velocity is a function only of some initial energy per unit charge mass, E , stored in the explosive gases, and the charge mass to casing mass ratio, C/M .

For case A (Figure A-1), consider a piston at distance l from a stationary wall and an arbitrary surface at distance x from the wall. Since pressure is assumed invariant with respect to x , the mass of gas between the arbitrary surface and the piston, and that between the surface and the wall, must be constant. If the pressure is invariant so is the specific volume, and, hence, the ratio of the volume behind the surface to the total volume is constant, or:

$$\frac{Ax}{Al} = \frac{x}{l} = C_1$$

where A is the area of the piston and C_1 is a constant independent of time.

If l_0 is the initial distance from the piston to the wall and x_0 the initial distance from the surface to the wall, then:

$$C_1 = \frac{x_0}{l_0}$$

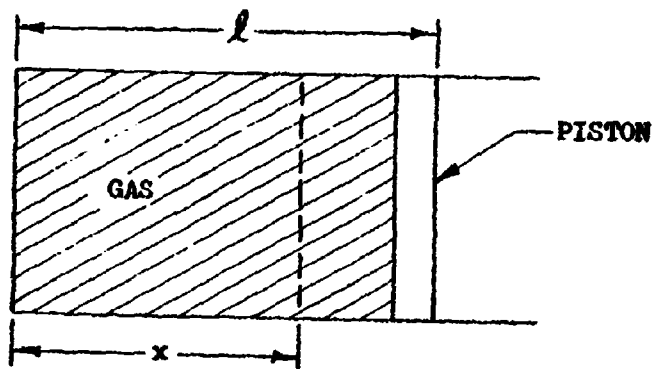


Figure A-1. Schematic Representation for One Dimensional Expansion Process.

and:

$$\begin{aligned}
 l &= l_0 + \int V(t)dt \\
 x &= C_1 l = \frac{x_0 l}{l_0} \\
 &= x_0 + \frac{x_0}{l_0} \int V(t)dt = x_0 + \frac{x}{l} \int V(t)dt \\
 &= x_0 + \int \frac{x}{l} V(t)dt = x_0 + \int V_x(t)dt
 \end{aligned}$$

where $V_x(t)$ is the velocity of the surface. Thus, we have:

$$V_x(t) = \frac{x}{l} V(t) \quad (\text{A-1})$$

which implies that the velocity of the gas is a linear function of the distance from the back wall, with maximum velocity equal to the velocity of the piston.

Case B (Figure A-2), considers a uniformly expanding cylinder of unit width. Using the same arguments presented above, the following development results:

The volume of gas from the center to r is:

$$v_r = \pi r^2$$

and the total volume is:

$$v_t = \pi R^2$$

and:

$$\frac{v_r}{v_t} = \frac{\pi r^2}{\pi R^2} = \frac{r}{R} = C_2$$

$$R = R_0 + \int V(t)dt$$

$$\begin{aligned}
 r &= C_2 R = r_0 + \int \frac{r}{R} V(t)dt \\
 &= r_0 + \int V_r(t)dt
 \end{aligned}$$

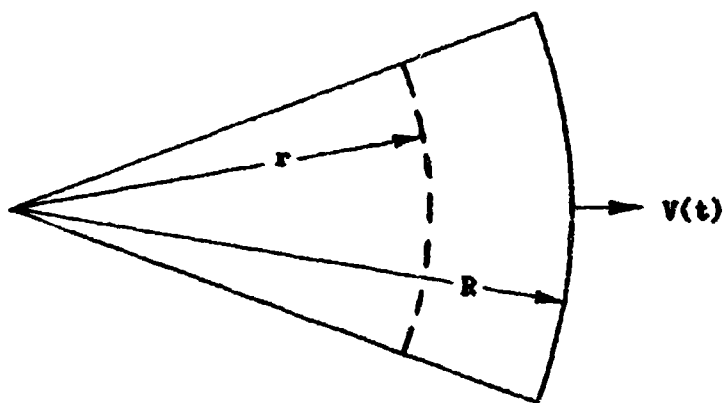


Figure A-2. Schematic Representation for Two Dimensional or Cylindrical Expansion Process.

where $V_r(t)$ is the velocity of the surface, thus:

$$V_r(t) = \frac{r}{R} V(t) \quad (A-2)$$

which again implies that the velocity of the gas is a linear function of the distance from the center to the casing.

Case C is quite similar to case B, the only difference being in the expressions for the volumes, v_r and v_t .

$$v_r = \frac{4}{3} \pi r^3$$

$$v_t = \frac{4}{3} \pi R^3$$

and:

$$\frac{v_r}{v_t} = \frac{\frac{4}{3} \pi r^3}{\frac{4}{3} \pi R^3} = \frac{r}{R} = C_3$$

which leads to the same result, i. e., the velocity of the surface is a linear function of the distance from the center to the casing.

Gurney assumes this linear velocity relationship, and it may be seen that this implies a uniform pressure with respect to linear distance. Further, it is seen that in the Gurney formula the detonation front is assumed plane in Case A, cylindrical (line initiation) in case B, and spherical (point initiation) in case C.

In accordance with assumption 3 above, assume that the initial energy, E , is converted entirely to kinetic energy in the gas and casing at the moment of breakup. If the breakup velocity of the case, and hence fragments, is V_B , then the energy in the case is:

$$E_c = 1/2 M V_B^2$$

where M is the mass of the case.

The kinetic energy in the gas is found by integrating the expression for kinetic energy over the volume of the gas:

$$E_g = \int_v \frac{V_g^2}{2} \rho_g dv$$

where ρ_g is the density of the gas and V_g is the velocity of the differential element. Since the assumption was made that V_g is proportional to linear distance, the equation for E_g may be written as:

$$E_g = \frac{V_B^2 \rho_g}{2R^2} \int_0^R r^2 dv$$

where r is the linear distance from gas at rest to gas at the casing, and R is the distance to the casing. Now if the total charge energy $CE = E_g + E_c$, then:

$$CE = \frac{1}{2} V_B^2 \left[M + \frac{\rho_g}{R^2} \int_0^R r^2 dv \right]$$

or:

$$V_B = \sqrt{2E} \sqrt{\frac{C}{M + \frac{\rho_g}{R^2} \int_0^R r^2 dv}}$$

For case A;

$$\frac{\rho_g}{l^2} \int_0^l x^2 A dx = \frac{\rho_g A l}{3} = \frac{C}{3}$$

where C is the charge mass, and:

$$\begin{aligned} V_B &= \sqrt{2E} \sqrt{\frac{C}{M + \frac{C}{3}}} \\ &= \sqrt{2E} \sqrt{\frac{\frac{C}{M}}{1 + \frac{1}{3} \frac{C}{M}}} \end{aligned}$$

(A-3)

For case B:

$$\frac{\rho_g}{R^2} \int_0^R r^2 2\pi r dr = \frac{\rho_g \pi R^2}{2} = \frac{C}{2}$$

or:

$$\begin{aligned}
 v_B &= \sqrt{2E} \sqrt{\frac{C}{M + \frac{C}{2}}} \\
 &= \sqrt{2E} \sqrt{\frac{C/M}{1 + 1/2 C/M}}
 \end{aligned}
 \tag{A-4}$$

For case C:

$$\frac{\rho_g}{R^2} \int_0^R r^2 4\pi r^2 dr = \frac{\frac{4}{3} \pi R^3 \rho_g (3)}{5} = \frac{3}{5} C$$

or:

$$\begin{aligned}
 v_B &= \sqrt{2E} \sqrt{\frac{C}{M + \frac{3}{5}C}} \\
 &= \sqrt{2E} \sqrt{\frac{C/M}{1 + \frac{3}{5}C/M}}
 \end{aligned}
 \tag{A-5}$$

Equations 3, 4, and 5 are the Gurney equations for piston, cylindrical, and spherical expansions, respectively. Note that although no information is available as to direction or fragment size, the initial velocity predicted should be as accurate as the value of E used in the equations.

A possible means of calculating the value $\sqrt{2E}$ follows.

Assume a simple equation of state, i. e., for an ideal gas:

$$Pv^\gamma = \text{constant}$$

The energy necessary to compress a unit mass of gas from an initial state P_0, v_0 to a final state P, v is calculated, where P is pressure and v the volume (specific volume for unit mass). If an arbitrary volume having uniform pressure throughout is assumed (Figure A-3), then the work done in compressing the volume through a differential volume is:

$$dw = Fdr = PAdr = Pdv = \frac{P_0}{v_0^{-\gamma}} v^{-\gamma} dv$$

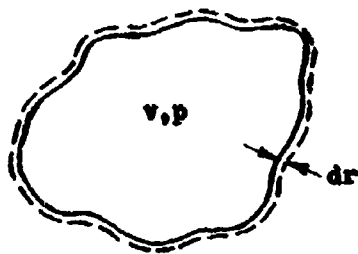


Figure A-3. Schematic Representation for Three Dimensional or Spherical Expansion Process.

and the total work done on the gas in compressing from P, v to P_0, v_0 is:

$$W = \frac{P_0}{v_0^{-\gamma}} \int_v^{v_0} v^{-\gamma} dv = \frac{-1}{\gamma-1} \left[P_0 v_0 - \frac{P_0 v^{1-\gamma}}{v_0^{-\gamma}} \right]$$

$$= \frac{-1}{\gamma-1} \left[P_0 v_0 - Pv \right]$$

If $P_0 = 0$ (an expansion process in which the gas is allowed to expand to infinity) then the total energy of the gas is:

$$E_g = \frac{Pv}{\gamma-1}$$

Now assume an initial specific gravity for the explosive of 1.6. a value for $\gamma = 2.8$, and an initial pressure of 3×10^8 psf. Then:

$$v = \frac{32.2}{62.4(1.6)} = .322 \text{ ft}^3/\text{slug}$$

and:

$$E_{g0} = \frac{(3 \times 10^8) (.322)}{1.8} = .536 \times 10^8 \text{ ft}^2/\text{sec}^2$$

By assuming that the volume of explosive has doubled at breakup:

$$\frac{P}{P_0} = \left(\frac{v_0}{v} \right)^\gamma = (.5)^{2.8} = .1435$$

and:

$$E_g = (.536 \times 10^8) (2) (.1435) = .154 \times 10^8 \text{ ft}^2/\text{sec}^2$$

The difference between these two values is the amount of energy converted to kinetic energy (neglecting energy lost in plastic deformation of the case, radiation, etc.). Thus, the calculated value for $\sqrt{2E}$ for the conditions assumed is:

$$\sqrt{2E} = \sqrt{2(.536 - .154) 10^8} = 8700 \text{ ft./sec.}$$

This value is within the same order of magnitude as the value generally used in the Gurney equations.

TAYLOR'S THEORY FOR END INITIATED CYLINDERS

Imposing the conditions which allow only the detonation wave to travel through the materials, the equations for finding the velocity of the casing can be developed. To simplify this development, the coordinate system is moved with the detonation front, thus the pressure of the detonation products will not impart energy to the casing, but an element of the casing will follow an equilibrium path in which the centrifugal force is balanced by the instantaneous pressure of the gas products. For a plane perpendicular to the axis of the cylinder and at a distance Z behind the detonation front, the equation which represents this balance can be written as:

$$2\pi r p = mD \frac{d\theta}{dt} = mD^2 \cos \theta \frac{d\theta}{dZ} \quad (A-6)$$

where m = mass per unit length of cylinder

p = instantaneous pressure

r = instantaneous inside radius

D = detonation velocity of the explosive

θ = angle of inclination of the wall with respect to the cylinder axis

t = time

at $t = 0$; Z and $\theta = 0$; $r = r_0$ and $p = p_0$.

With the proper trigonometric substitutions and coordinate conversion to a fixed observer, also assuming a steady-state condition, and employing the conservation of mass and momentum, gives an equation of the form:

$$\sin^2(\theta/2) = \frac{\pi \rho_0 r_0^2}{2mD} \left[\frac{p}{\rho(D-u)} - u \right] \quad (A-7)$$

where u = particle velocity associated with the detonation products

ρ = density of the detonation products

ρ_0 = density of the undetonated explosive.

The magnitude of the velocity is then given by:

$$V = 2D \sin \theta/2$$

or, using (A-7) above:

$$V = \left\{ \frac{2\pi\rho_0 r_0^2}{m} D \left[\frac{p}{\rho(D-u)} - u \right] \right\}^{\frac{1}{2}} \quad (\text{A-8})$$

The direction of the velocity vector is given as $\delta = 1/2 \theta$. Numerical values can be obtained by evaluating the pressure, density and particle velocity as a function of the radius of the expanding cylinder. If the detonation products behave as an ideal polytropic gas, the pressure and density during an adiabatic process are related by:

$$p = a\rho^\gamma$$

and, for an idealized detonation wave, the following equations must be satisfied:

$$\rho_0 D = \rho_1 (D - u_1)$$

$$p_1 = \rho_0 (D u_1)$$

$$D = c + u_1$$

$$c^2 = (dp/d\rho)$$

this gives five equations in eight unknowns, which can be solved if three of the unknowns are specified. The initial explosive density and the detonation velocity have been found experimentally for several different explosives, and it has been found that a value for γ of 2.7 to 3.0 is a good approximation, therefore, providing the necessary requirements for solution of equation (A-8).

CYCLONE PROGRAM (VON NEUMANN, STERNBERG, ET AL)

Problems involving transient shock dynamics and phenomena arising in the flow of compressible fluids have been solved by numerical procedures, and for a complete analysis a high speed computer is usually required. Von Neumann described a method for treatment of shocks so that the normal discontinuity identified with shocks can be replaced with a rapid but continuous change across the shock front. In the calculations, artificial dissipative terms are introduced into the

equations which give very nearly the correct velocity through the material and across the thin layers describing the shock. The proper change in pressure, density, temperature, etc., can also be provided. The Rankine-Hugoniot equations for the boundary conditions are satisfied if the dimensions of the shock layer are small compared with other relevant physical dimensions. The flow of the metal, as well as the gases, can be found and as a result the shape and velocity of the case at any time can be determined.

In applying the Von Neumann-Richtmyer method for a cylinder and employing the finite difference method discussed in Reference 11, the various materials are divided into zones with respect to a given coordinate axes.¹³ These zones are given Lagrangian coordinates which move with respect to the fixed coordinate system. If the fixed coordinate system is given by R , Z , and the Lagrangian coordinates given as k , l , then the equations of motion are given by;

$$\frac{d^2R}{dt^2} = \frac{-R}{\rho_0 R_0 A_0} \left[\frac{\partial P}{\partial k} \cdot \frac{\partial Z}{\partial l} - \frac{\partial p}{\partial l} \cdot \frac{\partial Z}{\partial k} \right]$$

$$\frac{d^2Z}{dt^2} = \frac{-R}{\rho_0 R_0 A_0} \left[\frac{\partial P}{\partial l} \cdot \frac{\partial R}{\partial k} - \frac{\partial p}{\partial k} \cdot \frac{\partial R}{\partial l} \right]$$

the energy equation is:

$$\frac{\partial E}{\partial t} = -P \frac{\partial V}{\partial t}$$

and the equation of state of each material present is of a form:

$$p = p(E, V)$$

ρ_0 = density of undetonated explosive

R_0 = initial radius of the cylinder

A_0 = initial areas of the zones in the explosive

P = pressure = $p + q$

V = specific volume

E = internal energy

q = artificial dissipative factor

$$\text{and } q = \frac{aA}{V V_0^2} \left(\frac{\partial V}{\partial t} \right)^2$$

where a is adjusted to give the desired sharpness to the shock.

The mass of each zone remains constant and the problem is one of determining the motion of the mass points associated with each zone. The acceleration of each mass point is determined from the pressures in the surrounding zones and for given time increments new velocity components, specific volumes, pressures and energies are computed for each zone.

The process starts at the initiation point of the explosive, and at the various time increments each zone is examined to determine if the detonation wave has reached it. If it has, the equation of state for the explosion products is used for the zone from that time on, otherwise the equation of state for the undetonated explosive is used for the zone. The time increments are computed by means of a stability criteria which insures that the total energy does not vary.

At the gas-metal boundary, problems arise because of velocity gradients in the materials. Therefore, a scheme to allow slippage at the boundary must be provided. The pressure must be continuous across the boundary, so an interpolation process is used which involves the pressures in both the gas and the metal. The motion of the metal and gas are then determined independently.

APPENDIX B

FLAT PLATE ANALYSIS

A technique similar to that used to analyze the center initiated cylinder is presented here for a flat plate where the explosive is initiated such that a plane wave impinges on the plate surface (Figure B-1).

Starting with the equation:

$$F = ma \text{ or } \frac{\rho \ell d^2x}{dt^2} = P = P_0 \left(\frac{x_0}{x}\right)^\gamma$$

(where ρ = density of the plate, ℓ = thickness of the plate and $\frac{d^2x}{dt^2}$ = acceleration). This represents the equation of motion of a unit area of material, and:

$$\frac{d^2x}{dt^2} = \frac{P_0}{\rho \ell} \left(\frac{x_0}{x}\right)^\gamma$$

$$\text{let } A = \frac{P_0}{\rho \ell} x_0^\gamma$$

$$\frac{d^2x}{dt^2} = \frac{A}{x^\gamma}$$

$$v = \frac{dx}{dt}, \quad \frac{d^2x}{dt^2} = \frac{d\left(\frac{dx}{dt}\right)}{dt} = \frac{dv}{dt} = \frac{dv}{dx} \frac{dx}{dt} = v \frac{dv}{dx}$$

$$\text{or } v dv = A x^{-\gamma} dx$$

$$v^2 = \frac{2A}{1-\gamma} x^{1-\gamma} + C_1$$

$$C_1 = v_0^2 + \frac{2A}{\gamma-1} x_0^{-(\gamma-1)}$$

$$v = \frac{dx}{dt} = \sqrt{C_1 - \frac{2A}{\gamma-1} x^{-(\gamma-1)}} = \sqrt{\frac{2A}{\gamma-1}} \sqrt{\frac{C_1(\gamma-1)}{2A} - x^{-(\gamma-1)}}$$

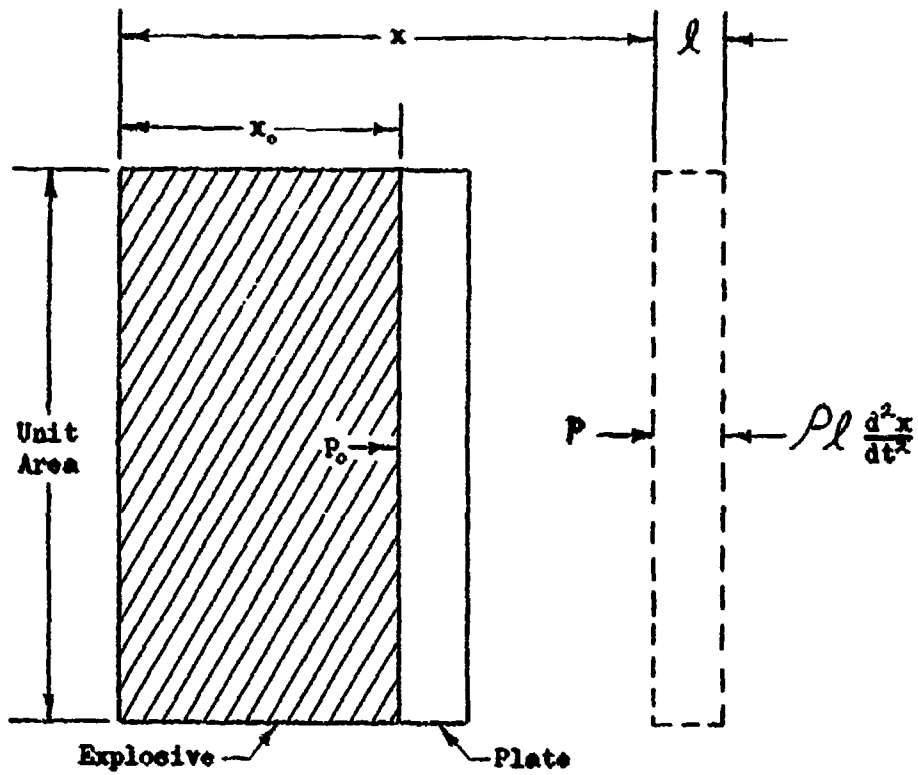


Figure B-1. Flat Plate Schematic.

$$\text{let } B = \sqrt{\frac{2A}{\gamma-1}} \quad \text{let } C = \frac{C_1(\gamma-1)}{2A} \quad \text{let } d = \gamma-1$$

$$\frac{dx}{dt} = B \left[C - x^{-d} \right]^{\frac{1}{2}}$$

$$dt = \frac{1}{B} \left[C - x^{-d} \right]^{\frac{1}{2}} dx$$

$$C = \frac{V_0^2 (\gamma-1) \rho t}{2P_0 x_0} + x_0^{-(\gamma-1)} = \frac{1}{x_0^\gamma} \left[\frac{V_0^2 (\gamma-1) \rho t}{2P_0} + x_0 \right]$$

Compare C to $x^{-(\gamma-1)}$, i. e., to $\frac{x}{x^\gamma}$, for $x \geq x_0$.

For $x \geq x_0$, C will always be greater than $x^{-(\gamma-1)}$ by an amount equal to:

$$\frac{V_0^2 (\gamma-1) \rho t}{2P_0 x_0^\gamma}$$

Use the binomial expansion theorem to expand the integrand and the integrate term by term.

$$B dt = \left[C^{-\frac{1}{2}} + \frac{1}{2} C^{-\frac{3}{2}} x^{-d} + \frac{1 \cdot 3}{2^2 \cdot 2} C^{-\frac{5}{2}} x^{-2d} + \frac{1 \cdot 3 \cdot 5}{2^3 \cdot 3} C^{-\frac{7}{2}} x^{-3d} + \dots \right] dx$$

$$B dt = D + x \left[C^{-\frac{1}{2}} + \frac{1}{2(1-d)} C^{-\frac{3}{2}} x^{-d} + \frac{1 \cdot 3}{2^2 \cdot 2! (1-2d)} C^{-\frac{5}{2}} x^{-2d} + \frac{1 \cdot 3 \cdot 5}{2^3 \cdot 3! (1-3d)} C^{-\frac{7}{2}} x^{-3d} + \dots \right]$$

$$t = D_1 + \frac{x}{B} \sum_{k=0}^{\infty} \frac{(2k)!}{2^{2k} (k!)^2 (1-kd)} C^{(k+\frac{1}{2})} x^{-kd}$$

at $t = 0$, $x = x_0$

$$D_1 = -\frac{x_0}{B} \sum_{k=0}^{\infty} \frac{(2k)!}{2^{2k} (k!)^2 (1-kd)} C^{-(k+\frac{1}{2})} x_0^{-kd}$$

Although analytical solutions have been obtained from the equations above for x and V as functions of t for the flat plate, a numerical integration technique may provide more expedient results.

A technique similar to that used for the cylinder is used to obtain plots of V vs. x (Figure B-2), x vs. t (Figure B-3), and V vs. t (Figure B-4). The assumptions are given below.

$$F' = \frac{1 - \left(\frac{x_0}{x}\right)^{\gamma-1}}{\gamma - 1}$$

$$K' = \frac{2P_0x_0}{\rho l}$$

$$V^2 = K'F' + V_0^2$$

$$P_0 = 2 \times 10^8 \text{ psf}$$

$$\rho = 15.25 \text{ slugs/ft}^3$$

$$x_0 = .125 \text{ ft}$$

$$l = .0417 \text{ ft}$$

$$\gamma = 3.0$$

$$x_0 \leq x \leq 1.5 x_0$$

$$F' = \frac{1 - \left(\frac{.125}{x}\right)^2}{2}$$

$$K' = \frac{4 \times 10^8 (.125)}{15.25 (.0417)} = 7.87 \times 10^7$$

$$V_t^2 = 78.7 F' + V_0^2$$

Using plots similar to the ones obtained above and by dividing the plate into concentric rings, the shape of a center initiated plate at various

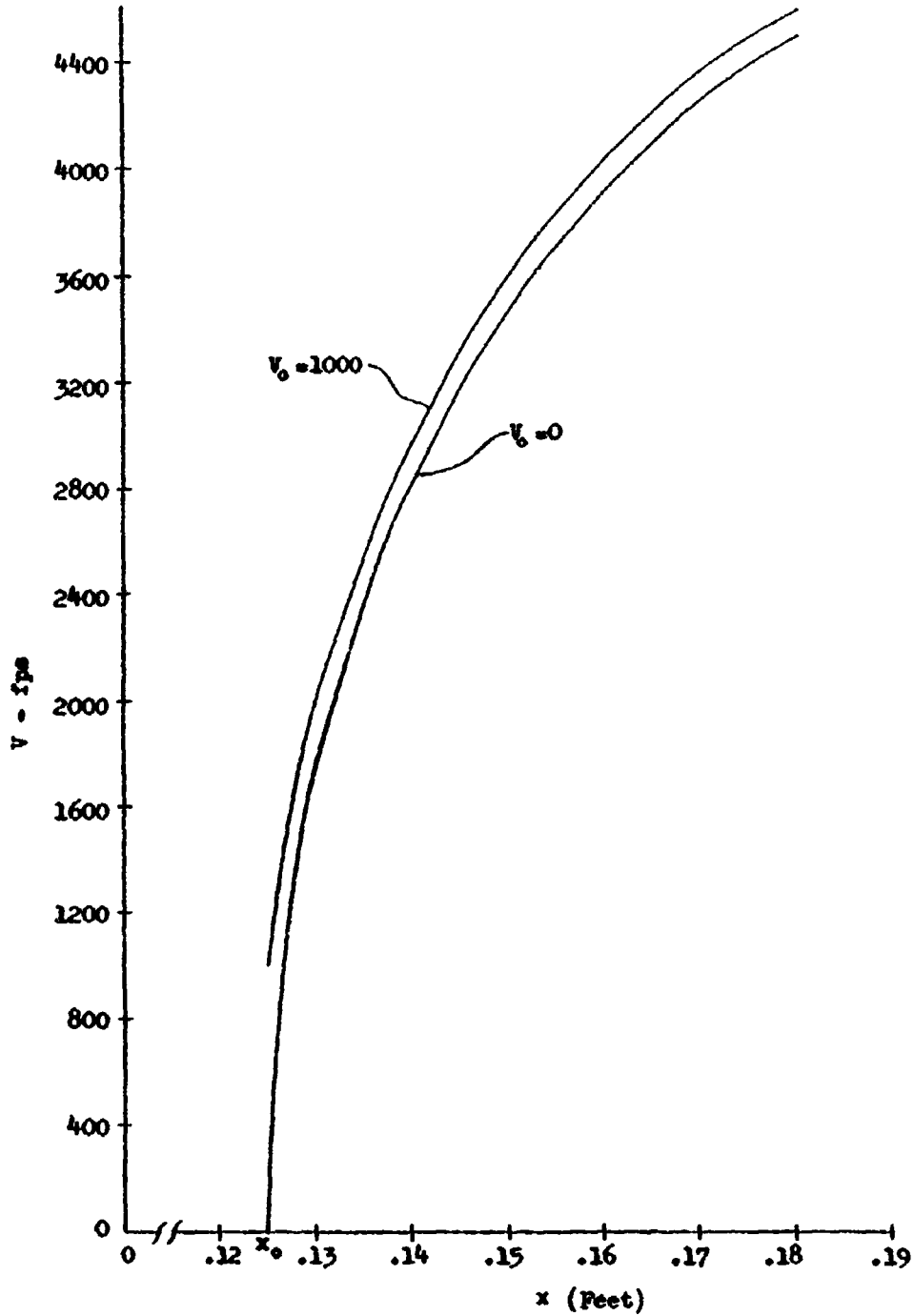


Figure B-2. Velocity of an Explosively Accelerated Flat Plate Versus Distance of Travel.

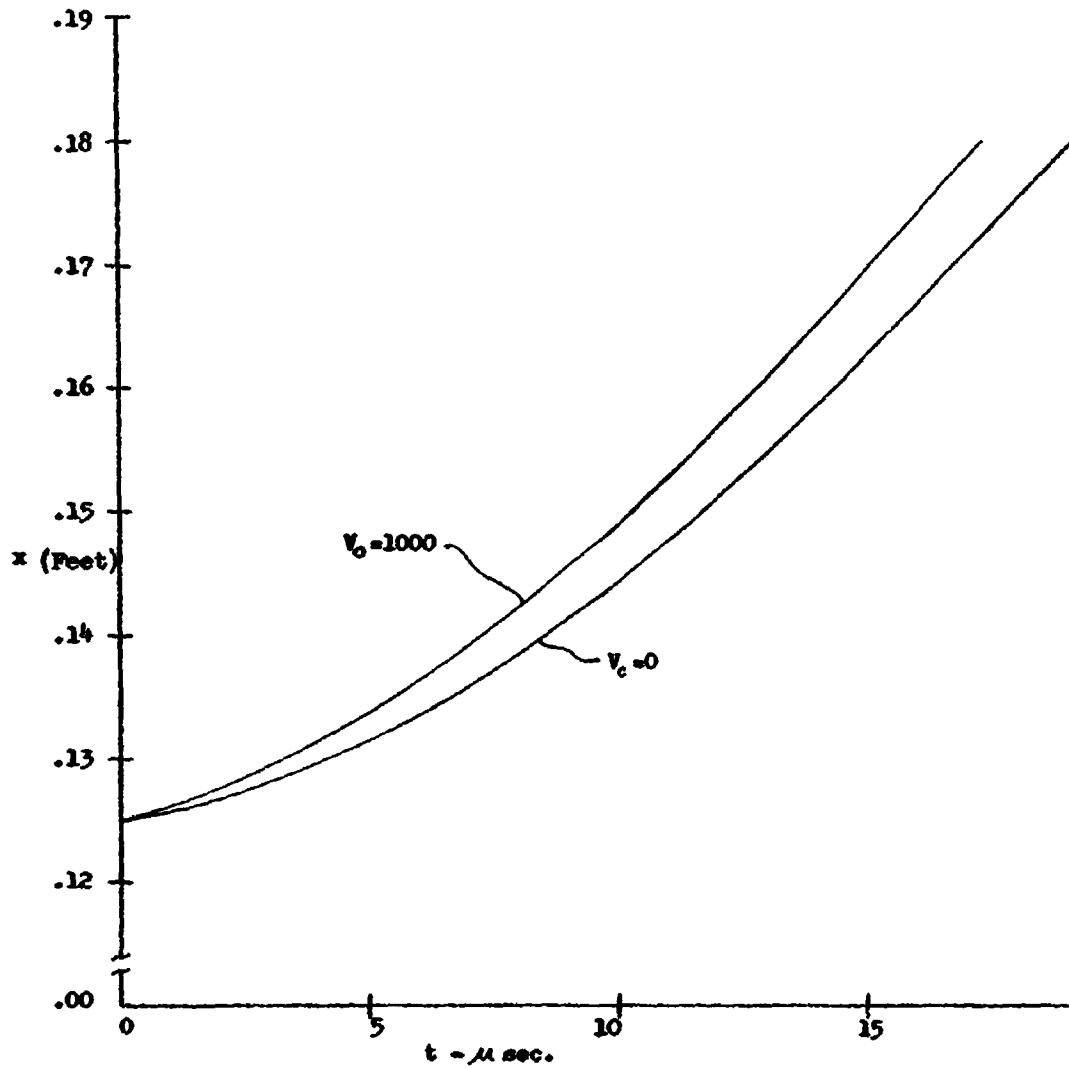


Figure B-3. Distance of Travel Versus Time for an Explosively Accelerated Flat Plate.

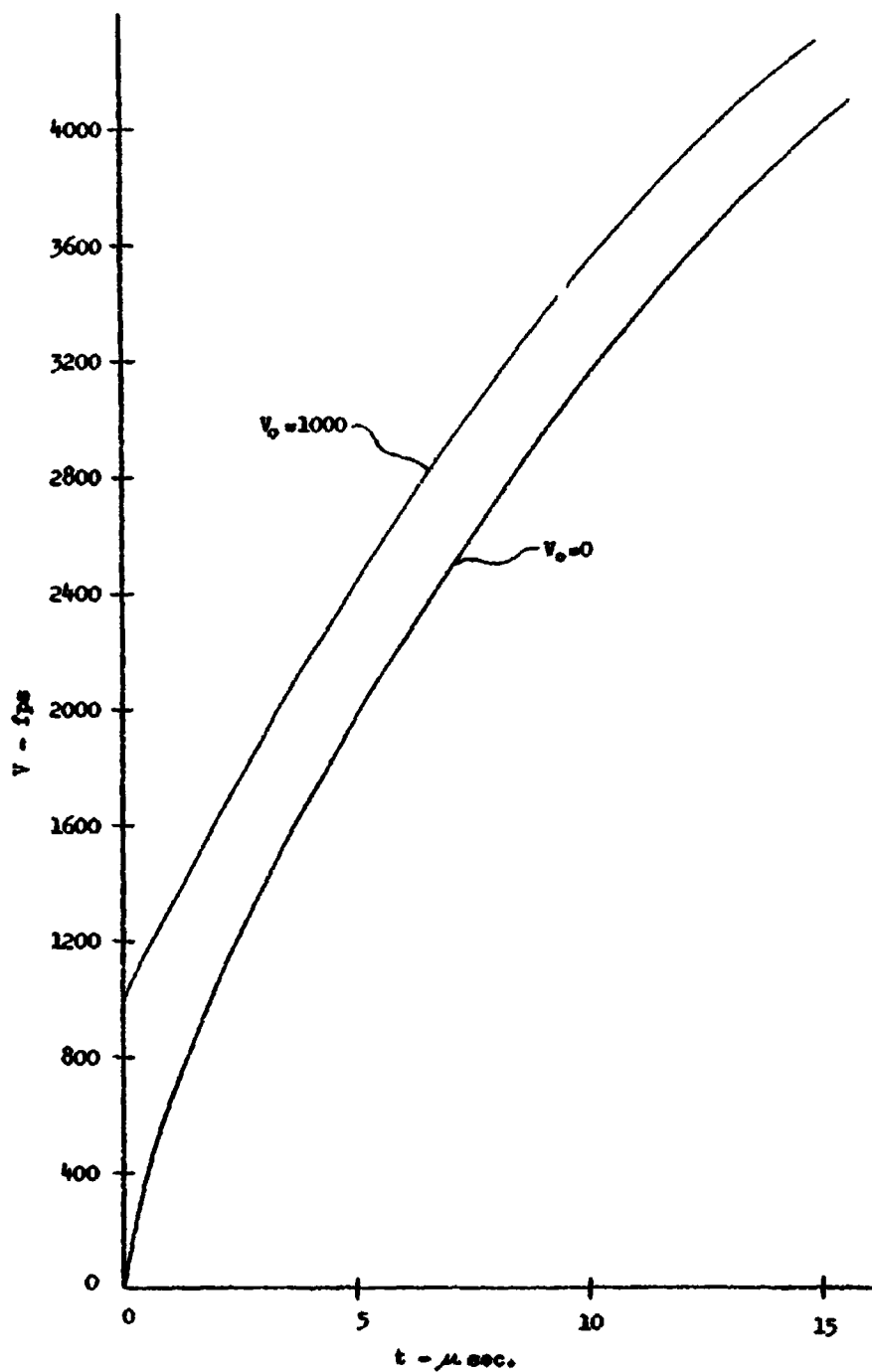


Figure B-4. Velocity of an Explosively Accelerated Flat Plate Versus Time.

times can be obtained (Figure B-5). The velocity vectors can then be determined from this plot and the strain analysis performed to predict the fragmentation of the plate.

To examine the effect of γ for this case, we again assume $V_0 = 0$, and the equation for V^2 reduces to:

$$V^2 = \frac{2P_0 x_0^\gamma}{\rho l (\gamma - 1)} x_0^{-(\gamma-1)} - x^{-(\gamma-1)} = \frac{2P_0 x_0}{\rho l (\gamma - 1)} \left[1 - \left(\frac{x_0}{x} \right)^{\gamma-1} \right]$$

$$= K' \left[\frac{1 - \left(\frac{x_0}{x} \right)^{\gamma-1}}{\gamma - 1} \right] = K' F'$$

where K' is a constant similar in form to the constant K found for the cylindrical case, and F' is a function of γ similar in form to the function F found for the cylindrical case. The same argument regarding γ will then apply to the flat plate.

Curves showing $\sqrt{F'}$ vs. x for various values of γ for the flat plate are shown in Figure B-6.

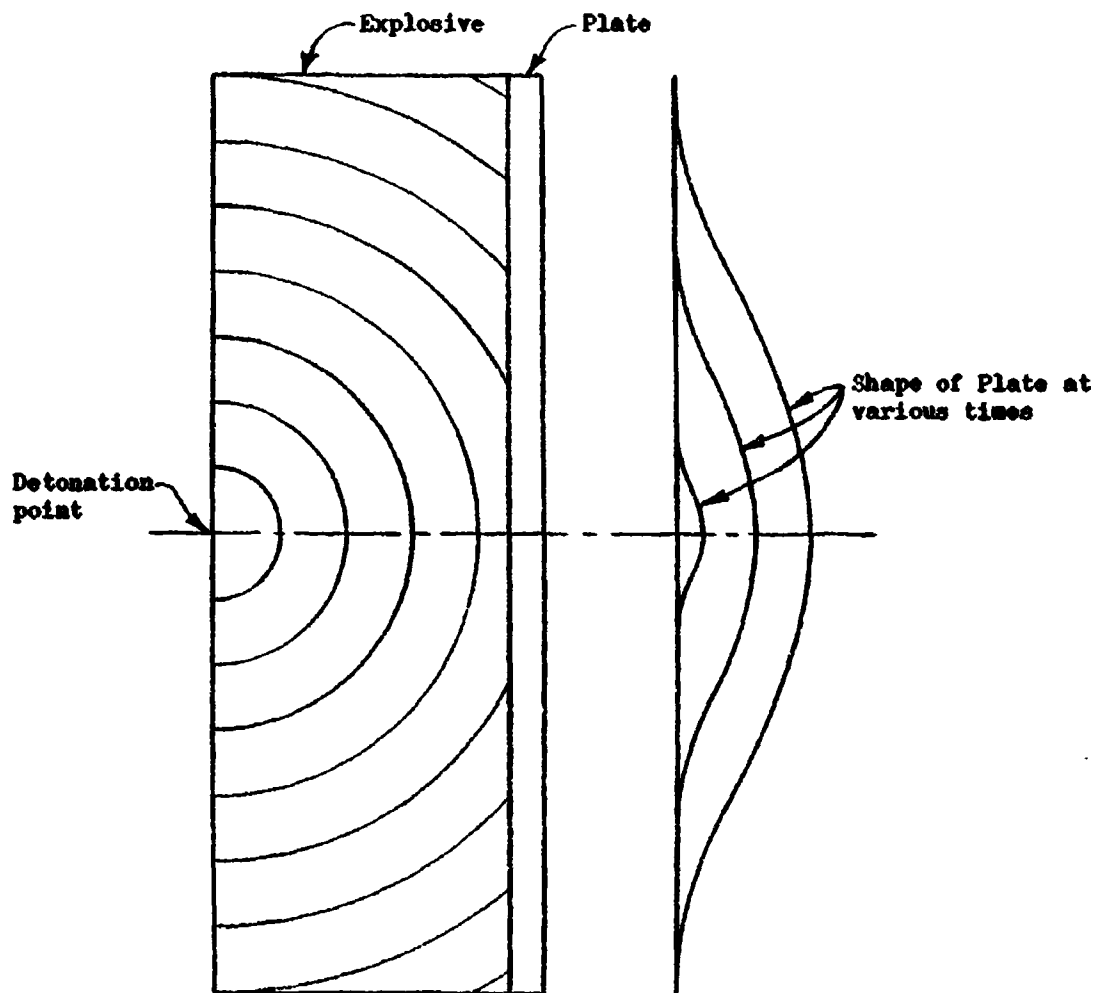


Figure B-5. Schematic of the Shape of a Flat Plate Due to Center Point Initiation of the Explosive.

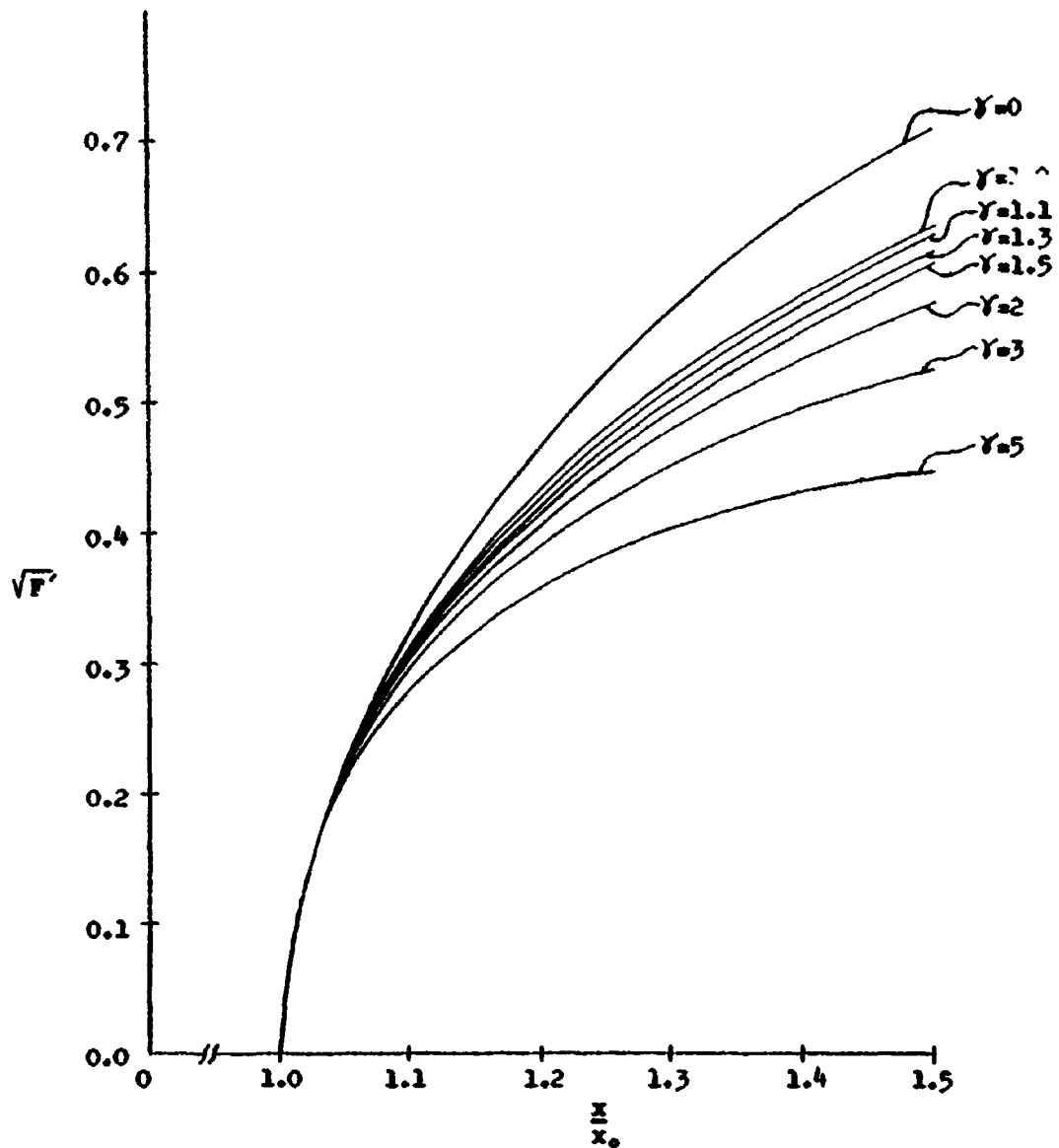


Figure B-6. Variation of the \sqrt{F} (Proportional to Velocity) Versus Distance of Travel of Flat Plate for Various Values of the Specific Heat Ratio (γ).

BIBLIOGRAPHY

1. Mott, N. F. , "Fragmentation of Shell Cases," Proceedings of Royal Society, London, Vol. 189, March - June, 1947.
2. Taylor, G. I. , "Analysis of the Explosion of a Long Cylindrical Bomb Detonated at One End," Scientific Papers of G. I. Taylor, Volume III. Cambridge University Press, 1963.
3. Gurney, R. W. , "Initial Velocities of Fragments from Bombs, Shell, and Grenades," BRL-405, September, 1943.
4. Sterne, T. E. , "A Note on the Initial Velocities of Fragments From Warheads," BRL-648, September, 1947.
5. Thomas, L. H. , "Theory of the Explosion of Cased Charges of Simple Shape," BRL-475, July, 1944.
6. Atkinson, G. W. , Thorn, E. M. , "A Method for Calculating the Initial Fragment Velocities from Hollow Warheads," NAVWEPS Report 8282, June, 1964.
7. Jones, E. E. , "Extension of Gurney Formulas," Honeywell Report No. M129, October, 1962.
8. Singh, Sampooran, "Proceedings of the Physical Society," (London) 1950.
9. Allison, F. E. , Watson, R. W. , Schriempf, J. T. , "Explosively Loaded Metallic Cylinders I & II," Journal of Applied Physics, Vol. 31, May, 1960.
10. Jones, H. , Taylor, G. I. , "Blast Impulse and Fragment Velocities from Cased Charges," Scientific Papers of G. I. Taylor, Vol. III. , Cambridge University Press, 1963.
11. Von Neumann, J. , Richtmyer, R. D. , "A Method for the Numerical Calculation of Hydrodynamic Shocks," Journal of Applied Physics, Vol. 21, March, 1950.
12. Gleyzal, A. , Sternberg, H. M. , Solem, A. D. , "Explosives Hydrodynamics Calculations," NOL, September, 1959.
13. Orlow, L. , Piacesi, D. , Sternberg, H. M. , "A Computer Program for the Analysis of Transient, Axially Symmetric, Explosion & Shock Dynamics Problems," NAVWEPS, Report 7265, December, 1960.

14. Clark, J. C. , Day, C. H. , "Flash Radiographs of Scale Model 20 lb. Fragmentation Bomb Immediately After Static Detonation," BRL Memo Report No. 396, October 2, 1945.
15. Clark, J. C. , Day, C. H. , "Flash Radiographs of Model Bombs During and Immediately Following Static Detonation," BRL Memo Report No. 363, April 18, 1945.
16. Dunn, D. J. , Jr. , "Some Notes on the Determination of Initial Fragment Velocity by Moving Picture Camera Method," BRL Memo Report No. 658, March, 1953.
17. Rinehart, J. S. , Pearson, J. , "Explosive Working of Metals," The Macmillan Co. , 1963.
18. Atkinson, G. W. , Nassengill, E. G. , "Calculating Initial Fragment Velocity from Penetration Data," NAVWEPS Report 8280, June, 1964.
19. Giere, A. C. , "Calculating Fragment Penetration and Velocity Data for Use in Vulnerability Studies," NAVWEPS Report 6621, October, 1959.
20. Thomas, L. H. , "Analysis of the Distribution on Mass, in Speed and in Direction of Motion, of the Fragments of the 90 mm A.A. Shell," BRL Report No. 434, December, 1943.
21. Lewy, H. , "Number, Angular Distribution and Velocity of Fragments from 105 MM Shell," BRL Report No. 386, July 28, 1943.
22. Thomas, L. H. , "On Determining Parameters for a Theoretical Formula to Best Fit an Observed Fragment Mass Distribution by the Method of Maximum Likelihood," BRL Report No. 552, June, 1945.
23. Gurney, R. W. , Sarmousakis, James N. , "The Mass Distribution of Fragments from Bombs, Shell, and Grenades," BRL Report No. 448, February, 1944.
24. Tomlinson, William R. , Jr. , "Application of a Derived Equation to Fragmentation Data," Picatinny Arsenal Report No. 1590, February, 1946.
25. Famiglietti, M. , "Fragmentation of Ring Type Cylindrical Shell Made of Various Metals," BRL Memo-Report 597, March, 1952.

DISTRIBUTION LIST

<u>Recipient</u>	<u>Number of Copies</u>
Commanding Officer Picatinny Arsenal Attn: Procurement & Production Directorate SMUPA-PB Dover, New Jersey	7
Defense Documentation Center Cameron Station Alexandria, Virginia 22314	10
Office of Technical Services Department of Commerce Washington 25, D. C. Attn: Acquisition Section	2
Denver Research Institute Files University of Denver Denver, Colorado 80210	11